



Synthèse de nanoparticules par ablation laser : principes – exemples – applications

Frédéric Dumas-Bouchiat^{1,2,3}

Corinne Champeaux¹, Alain Catherinot¹, Nora M. Dempsey^{2,3}, Dominique Givord^{2,3}

¹Univ Limoges, CNRS, SPCTS UMR 7315, Ctr Europeen Ceram, F-87068 Limoges, France

²Univ. Grenoble Alpes, Inst. Neel, F-38042 Grenoble , France

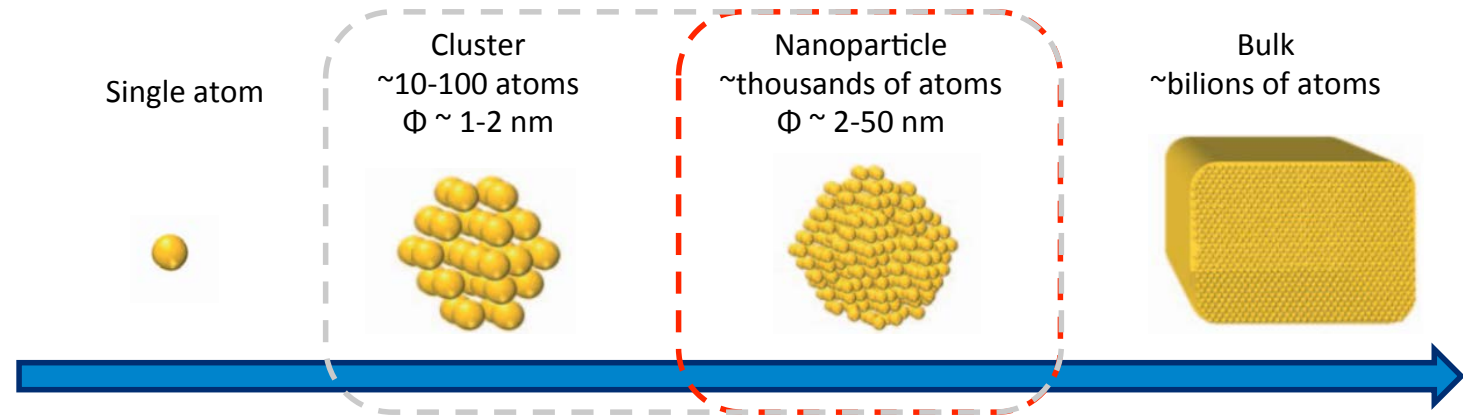
³CNRS, Inst NEEL, UPR2940 F-38042 Grenoble, France



Introduction to nanoparticles

Properties versus scales

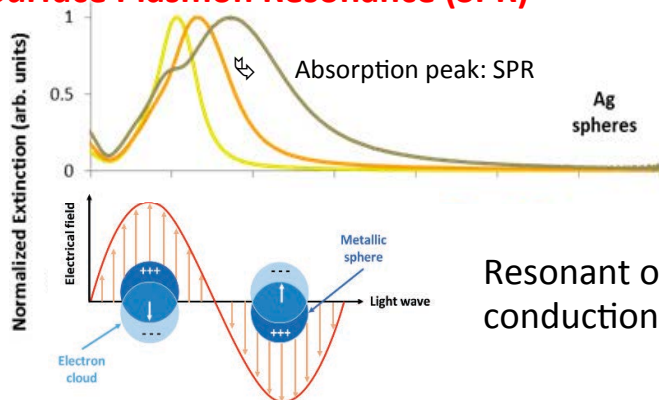
- Different properties at different scales



- Discrete electronic level vs Electronic band structure

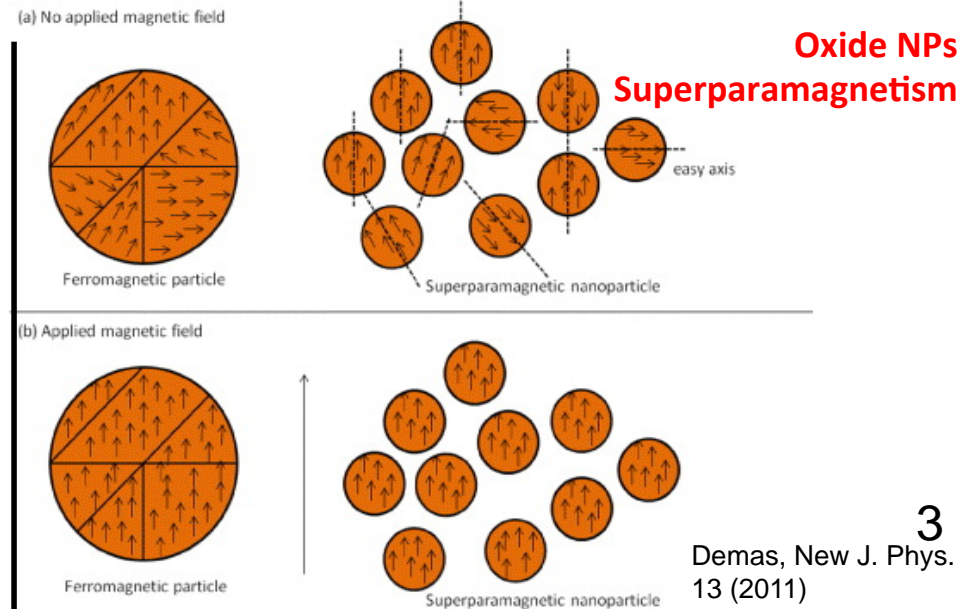


Metal. NPs Surface Plasmon Resonance (SPR)



Resonant oscillation of conduction e- stimulated by E

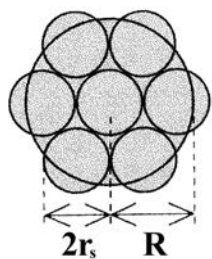
Oldenburg, Proc. SPIE 4810, Properties of Metal Nanostructures, 36 (2002)



3
Demas, New J. Phys. 13 (2011)

Some numbers

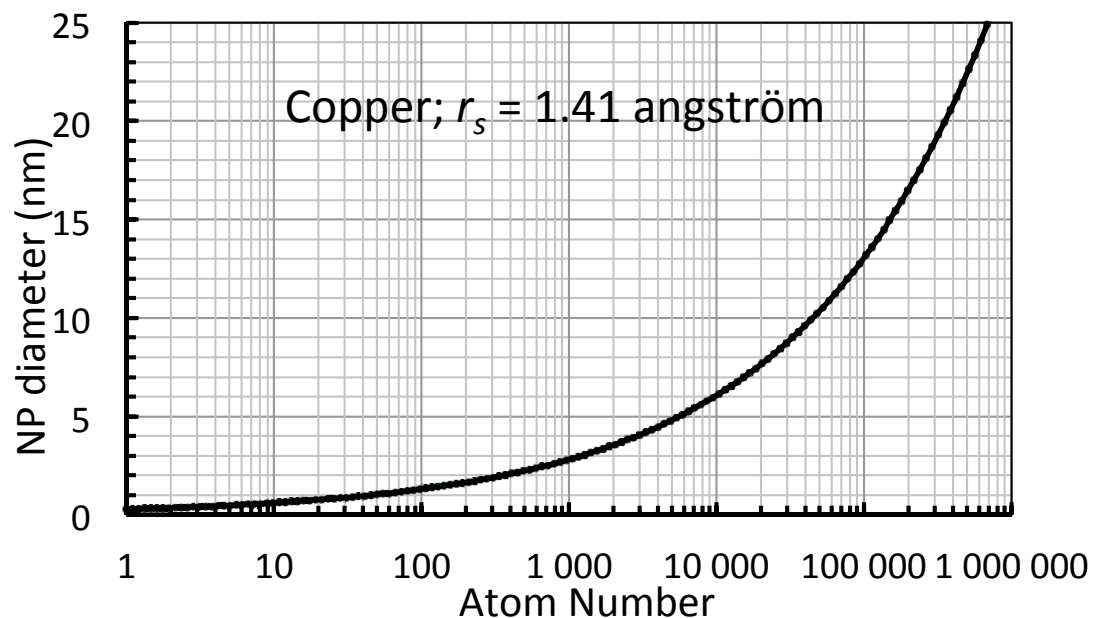
Hyp: spherical NP constituted by n atoms
 r_s Wigner-Seitz atomic radius



$$R = r_s \cdot n^{(1/3)}$$

Diameters

- ✓ 1 nm \approx 45 atoms
- ✓ 3 nm \approx 1 272 atoms
- ✓ 5 nm \approx 5 844 atoms
- ✓ 10 nm \approx 43 249 atoms



Ratio R $R = \frac{\text{Surface atoms}}{\text{Number of atoms in cluster}}$

Atoms number	13	55	147	309	561
(*)					
Number of shells	1	2	3	4	5
Number of atoms in cluster	M ₁₃	M ₅₅	M ₁₄₇	M ₃₀₉	M ₅₆₁
Percentage surface atoms	92%	76%	63%	52%	45%

2.3 nm \varnothing

(*) G. Schmid, Endeavour, Cluster and Colloids – Bridges Between Molecular and Condensed Material, **14** (1990)
 Aiken J. Mol. Catal. A: Chem. **145** (1999)

Homogeneous nucleation; vapor phase

Thermodynamic Approach

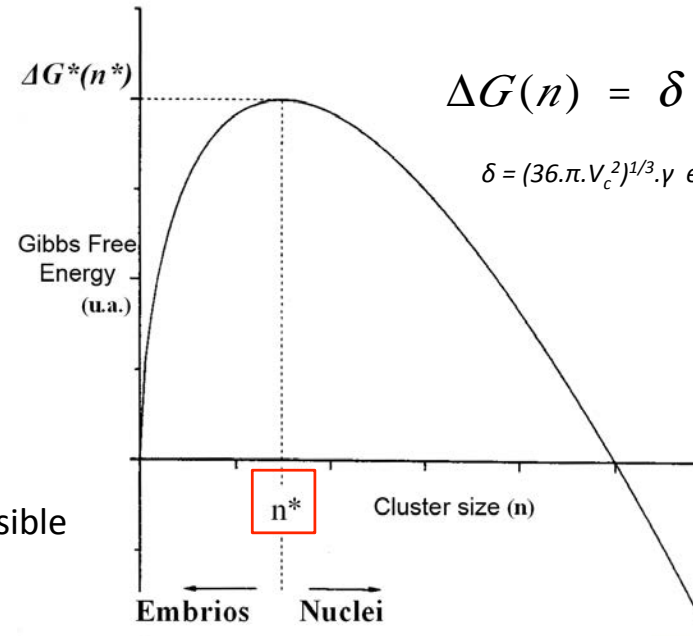
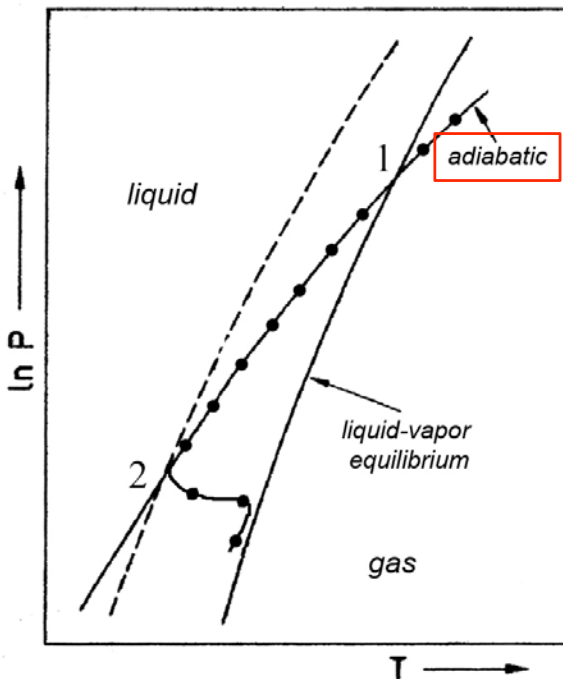
Free energy change

$$\Delta G(r) = 4 \cdot \pi \cdot r^2 \cdot \gamma + \frac{4}{3} \cdot \pi \cdot r^3 \cdot \Delta G_v$$

Surface free energy vs Volume free energy

$$\Delta G_v = -\frac{k \cdot T}{V_c} \cdot \ln \frac{P}{P_s}$$

- $S > 1$: Sursaturated vapor; Spontaneous nucleation possible
- $S < 1$: just vaporisation



$$\Delta G(n) = \delta \cdot n^{\frac{2}{3}} - k \cdot T \cdot \ln S \cdot n$$

$$\delta = (36 \cdot \pi \cdot V_c^2)^{1/3} \cdot \gamma \text{ et } k \cdot T \cdot \ln S = \Delta \mu \text{ chemical potential}$$

k : Boltzman Constante

T : nucleation Temperature

S : sursaturation rate

Sursaturation needed

$$S = P / P_s$$

- P vapor partial pressure, P_s saturated vapor pressure @ T_s
- T_s interface Temperature

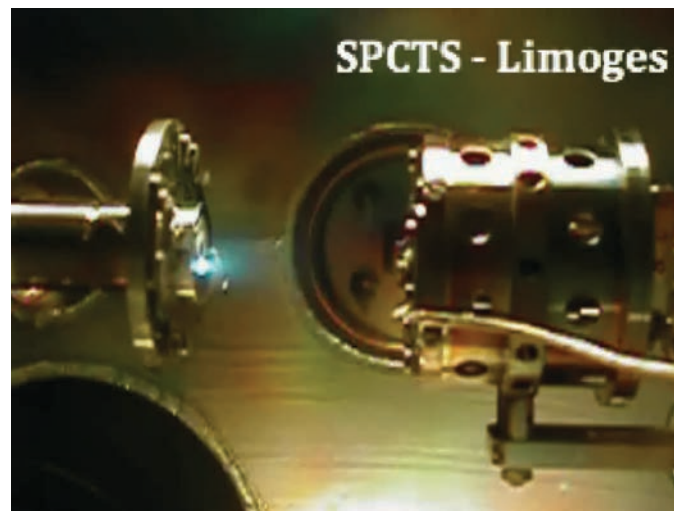
adiabatique expansion

Sursaturation conditions → gas under high pressure (He, thermal conductivity)

↪ supersonic beam

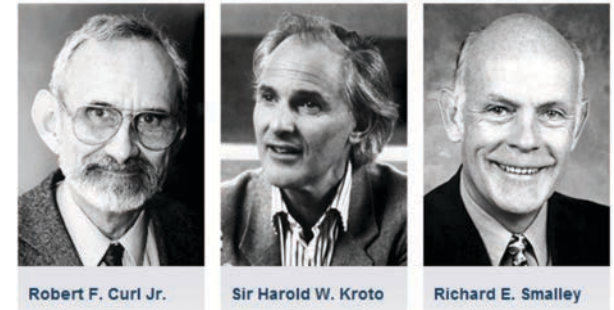
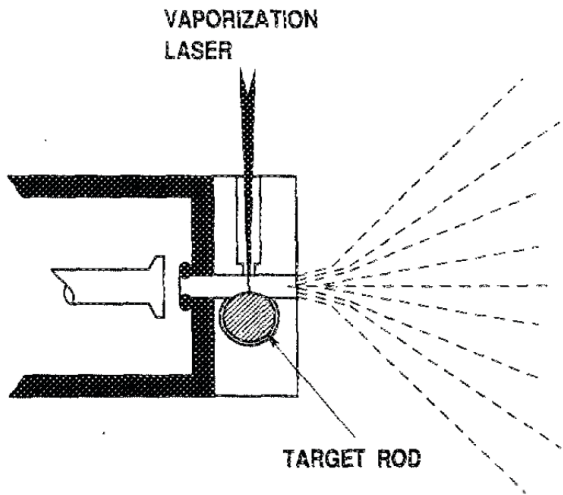
↪ specific process

Laser vaporisation sources: principe

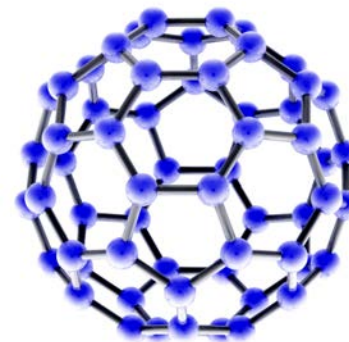
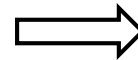
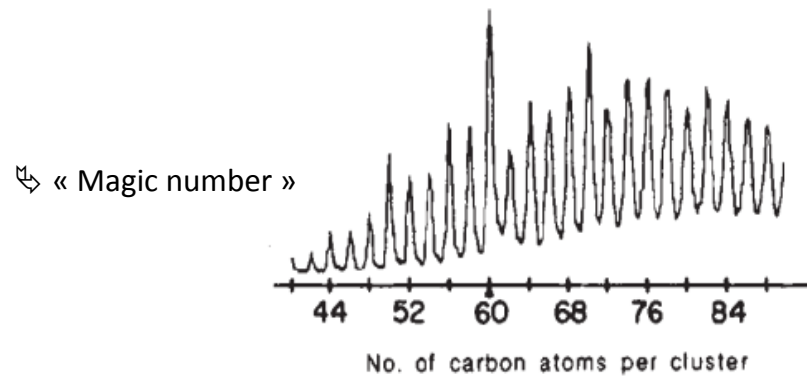


History – Smalley source

13^{ème} Journées – Réseau Plasmas Froids – La Rochelle – 17-20 octobre 2016

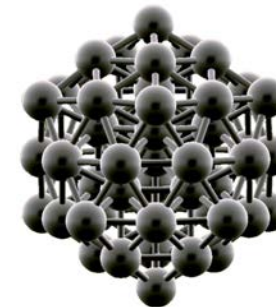
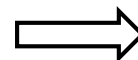


1996 Nobel Prize in Chemistry



NP composed of 60 Carbon Atoms (C₆₀ fulleren – Bucky Ball)

↪ Remark:



Ag Dense NP composed of 55 Silver Atoms

¹R.E. Smalley et al., J. Chem. Phys. 74(11) (1981)

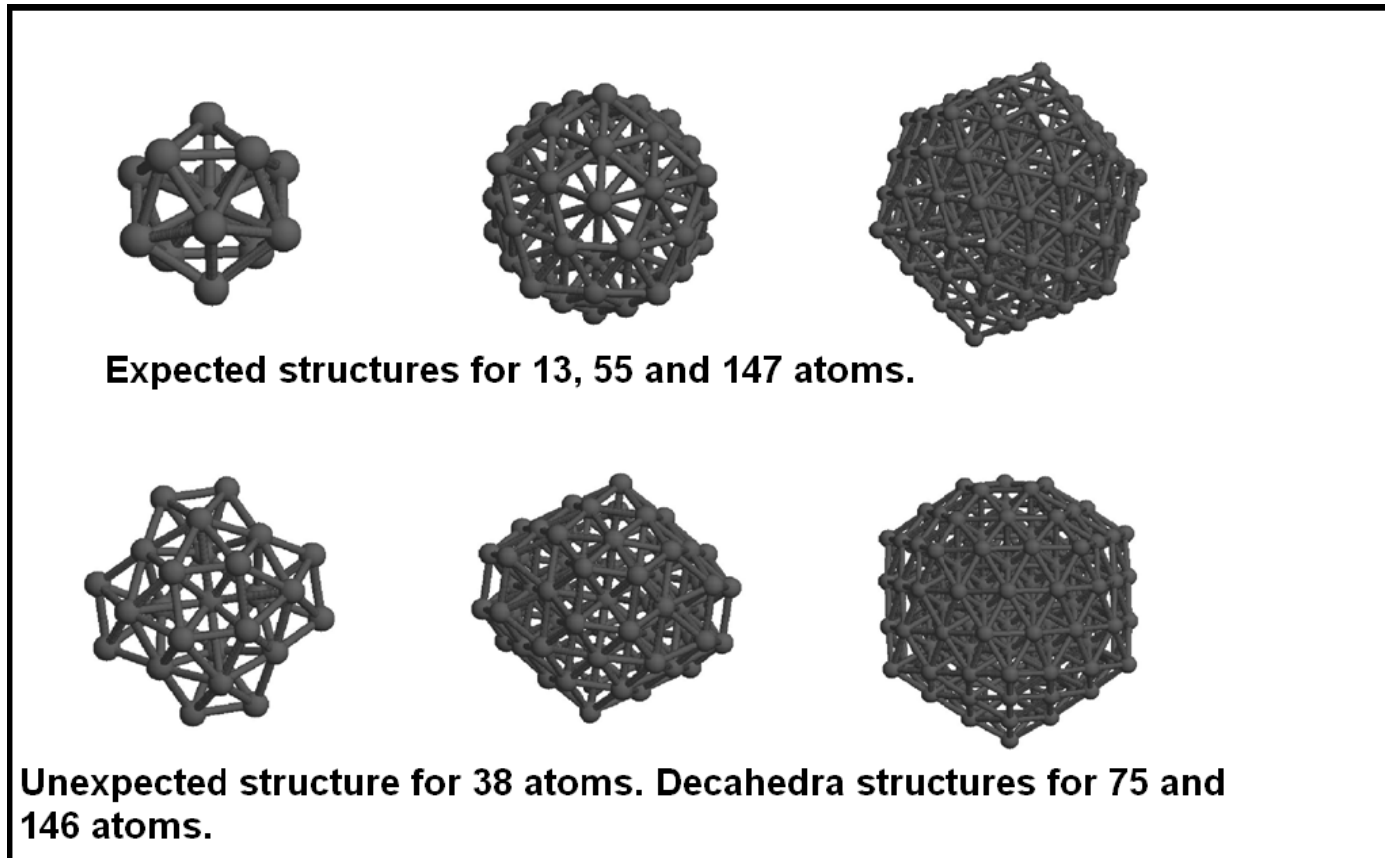
²R.E. Smalley, Laser Chem. 2 (1983)

³H. W. Kroto, J. R. Heath, S. C. O'Brien, R. F. Curl, and R. E. Smalley, "C₆₀: Buckminsterfullerene", Nature 318 (1985)

Cluster: Magic number

Molecular dynamics simulation, growth process of isolated Co clusters in gas phase

icosahedral



Structures

D4h symmetry

truncated icosahedral

Principle:

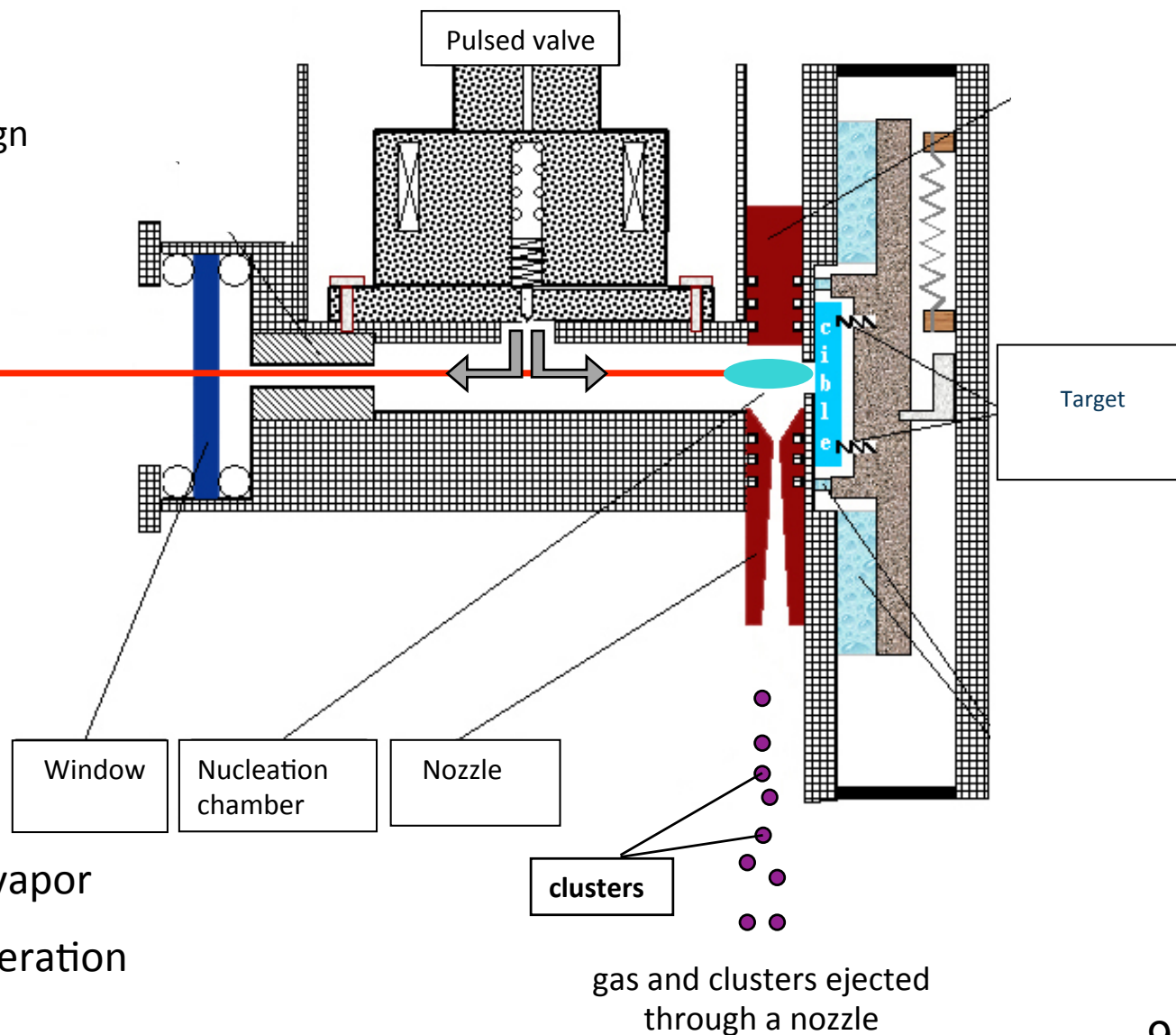
Cluster Beam Generator (CBG);
Laser Vaporisation Sources (LVS); Free Cluster Generator (FCG)

Principle :

Target vaporization with laser
Gas injected by a pulsed valve
Nucleation room from the design
of Milani-De Heer³

↳ Clusters growth control

YAG: 532nm

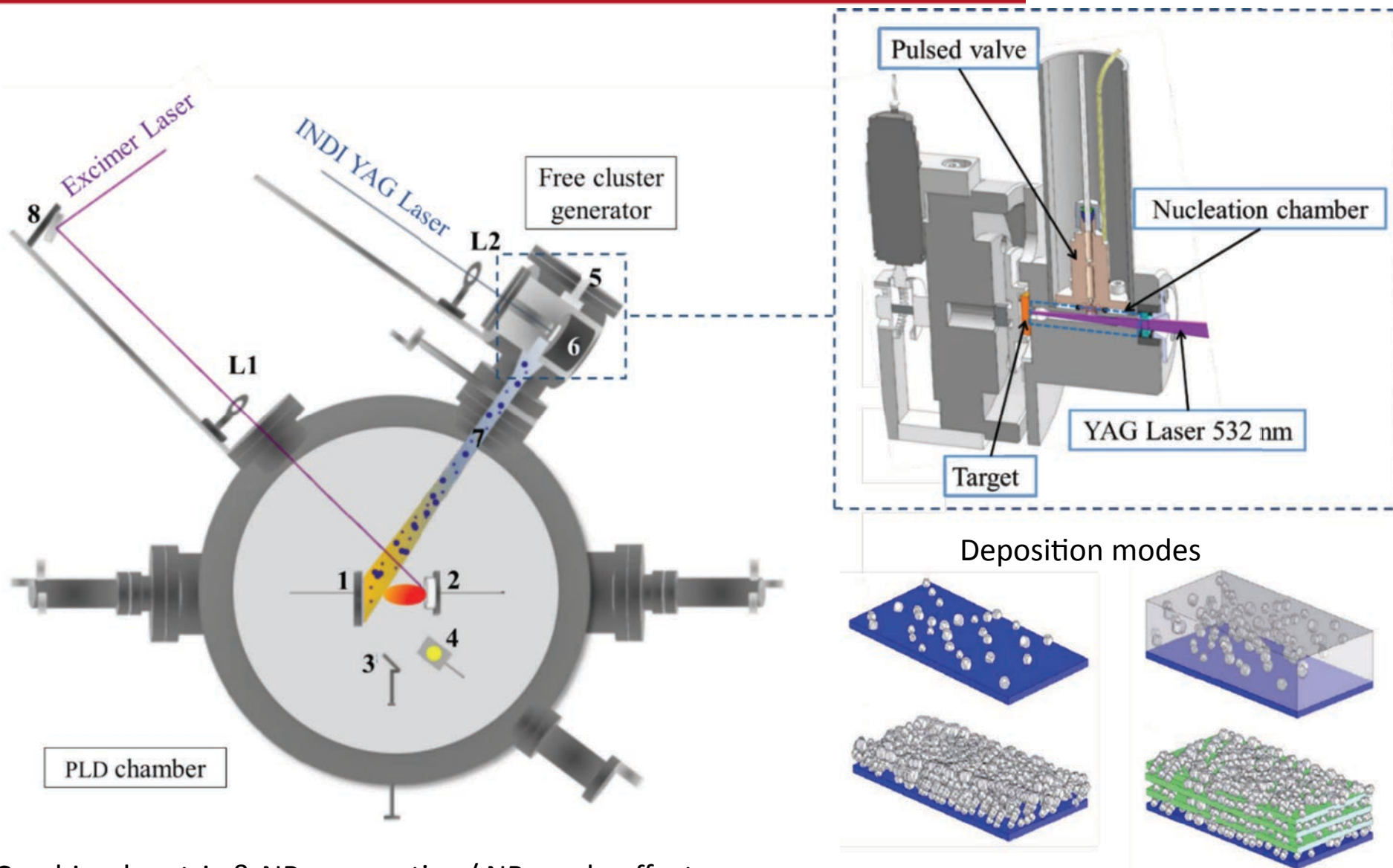


↳ synthesis of NPs in the vapor

↳ cluster (NPs) Beam Generation

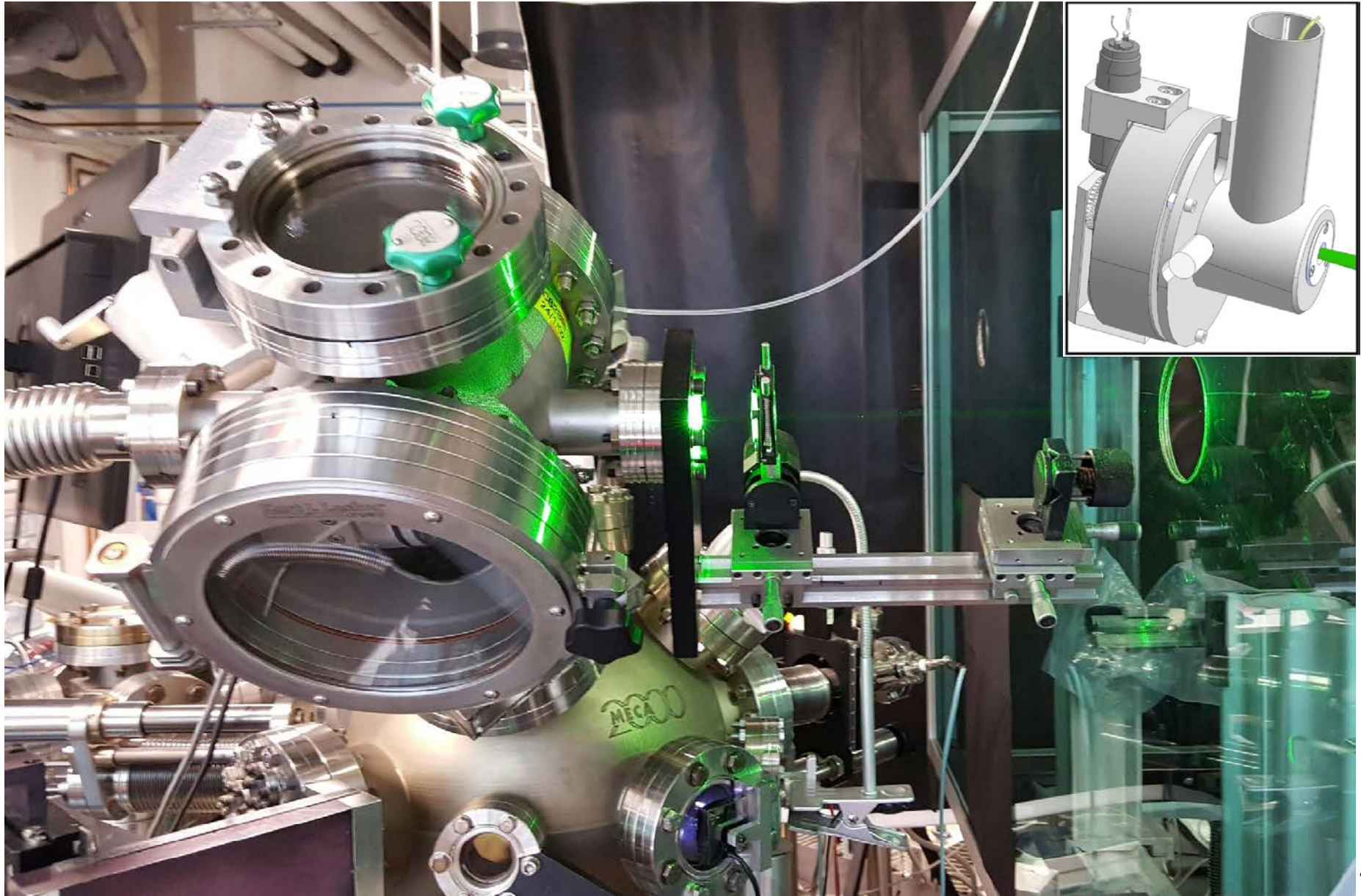
gas and clusters ejected
through a nozzle

NP Beam Generator (home made)



Combined matrix & NPs properties / NPs scale effect

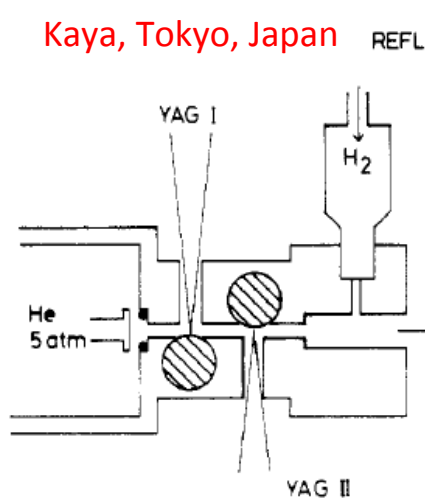
Limoges laser vaporisation source



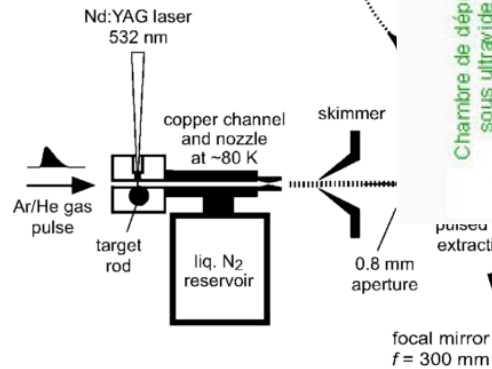
Smalley's childs

13^{ème} Journées – Réseau Plasmas Froids – La Rochelle – 17-20 octobre 2016

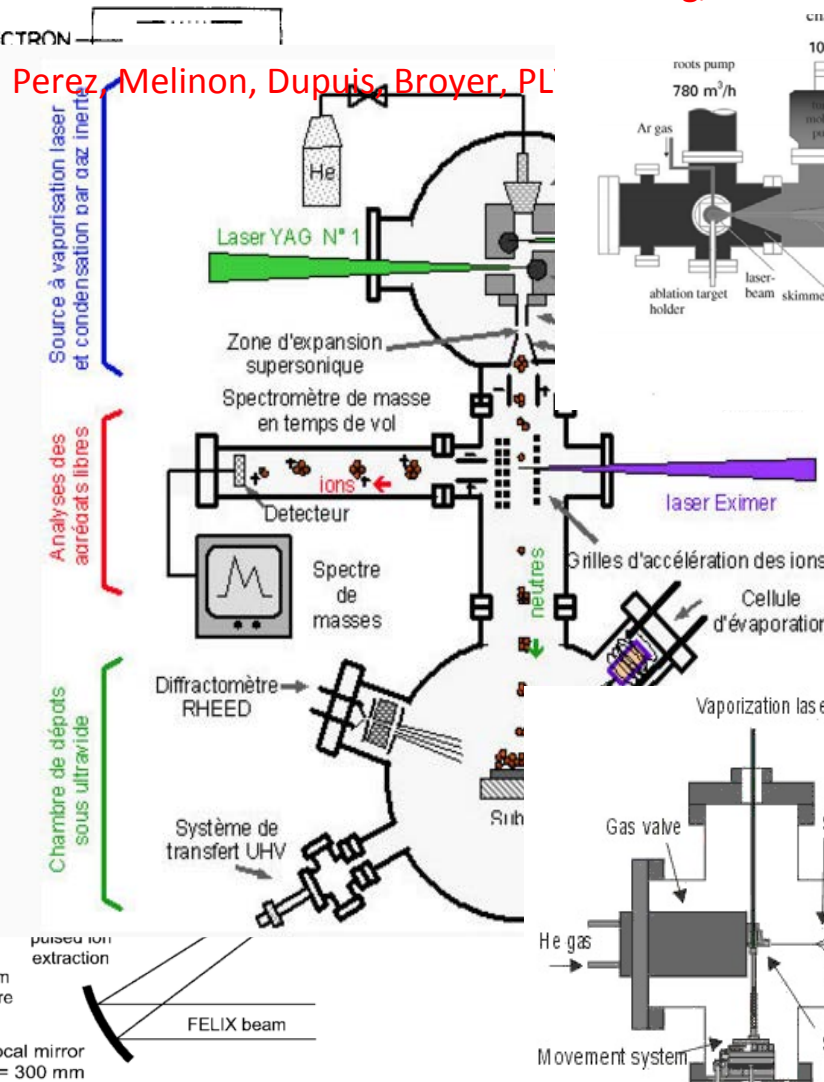
Kaya, Tokyo, Japan



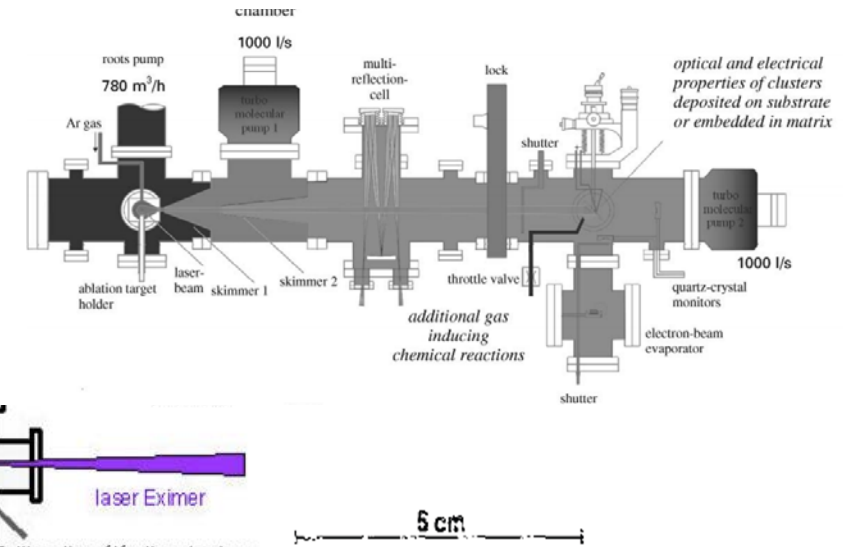
Fielicke, Nieuwegein, The Netherlands



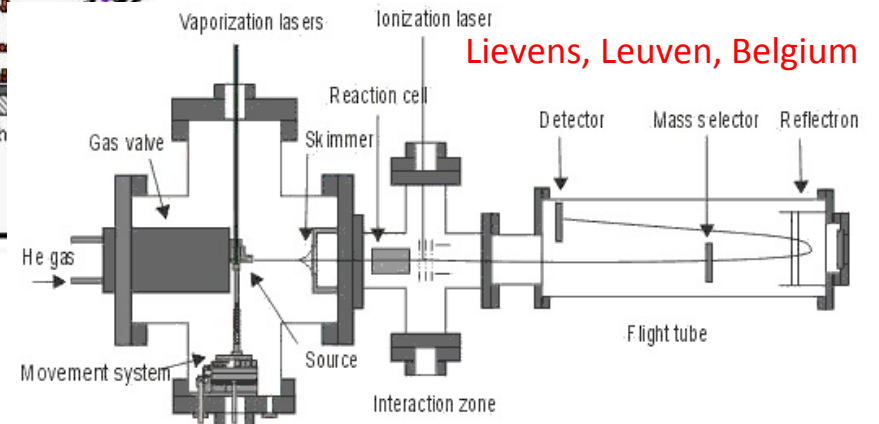
Perez-Melinon, Dupuis, Broyer, PL



Kreibig, Aachen, Germany



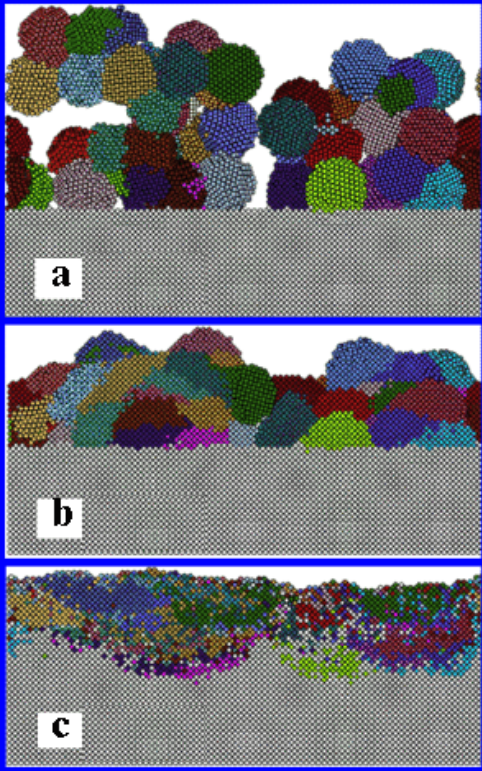
Lievens, Leuven, Belgium



Laser vaporization cluster source

Reflectron time-of-flight mass spectrometer

Modelling from Haberland et al. Mo NPs stacks on Mo substrate¹



- ↪ Cluster @ 0,1 eV/at:
keep their flying characteristics
Highly porous stacks of NPs (~50%)²
Weak adherence
 - ↪ Probability of NP fragmentation is weak
- ↪ Cluster @ 1 eV/at:
- ↪ Clusters @ 10 eV/at:
Dense « epitaxial » (Mo on Mo-substrate)

¹Haberland, Phys. Rev. B 51 (1995)

Approximation, overestimated cluster velocity :

NP velocity $V_{\max} \approx$ gas velocity $V_{\text{échappement}}$ (sound velocity v_{∞})
$$v_{\infty} = \frac{2k}{m_{He}} \left(\frac{\gamma}{\gamma - 1} \right) T = 1700 \text{ m/s (He)}$$

Cobalt NP :

Kinetic-E \approx 0.7 eV/at

Cohesion-E (bulk) \approx 4.5 eV/at

→ $E_{\text{cinétique}} \ll E_{\text{cohésion}}$

↪ NP keep their flying shape (shape memory)

²Dumas-Bouchiat, J. Appl. Phys. 100 (2006)

NP growth: homogeneous nucleation theory

Kinetic equations for NP-NP reactions:

$$\frac{dn_k^*}{d\tau(t)} = \sum_{\substack{i+j=k \\ i \leq j}} C_{ij}^* \cdot n_i^* \cdot n_j^* - \sum_i C_{ik}^* \cdot n_i^* \cdot n_k^*$$

Formation rate of k-sized NP resulting from the coalescence of a i-NP and a j-NP

Number of events where k-sized NPs form bigger NPs

C_{ij} : coalescence probability between a i-NP and a j-NP

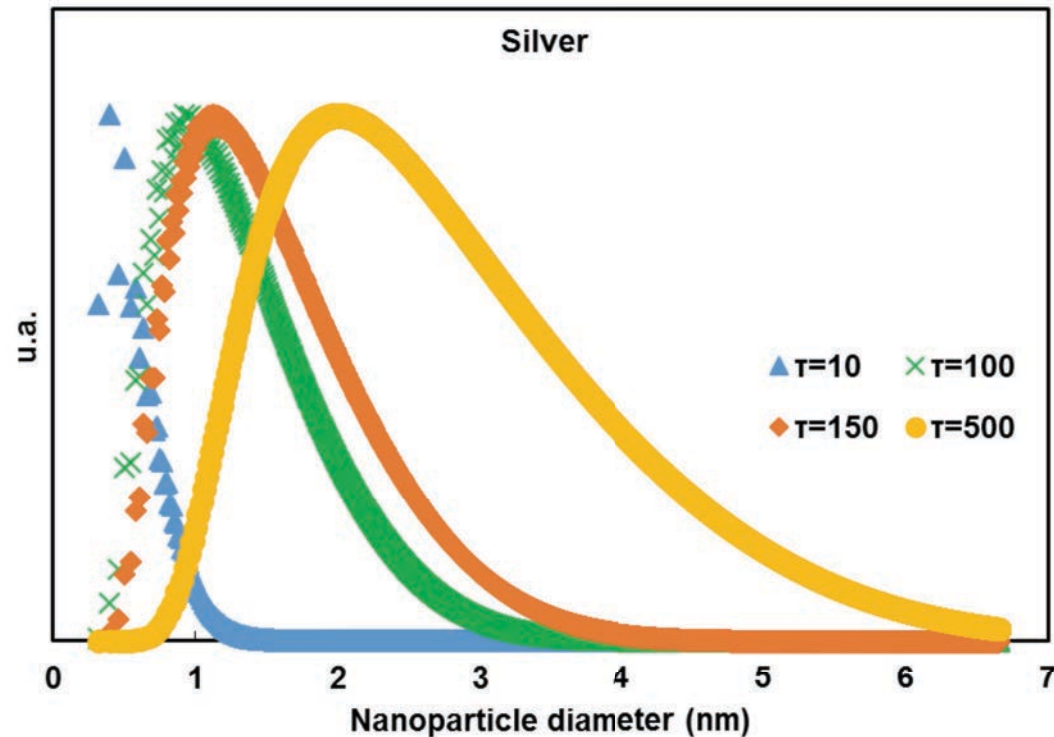
$$n_i^* = \frac{N_i}{N} \quad \text{reduced variable}$$

n_i^* : number of i-sized NPs

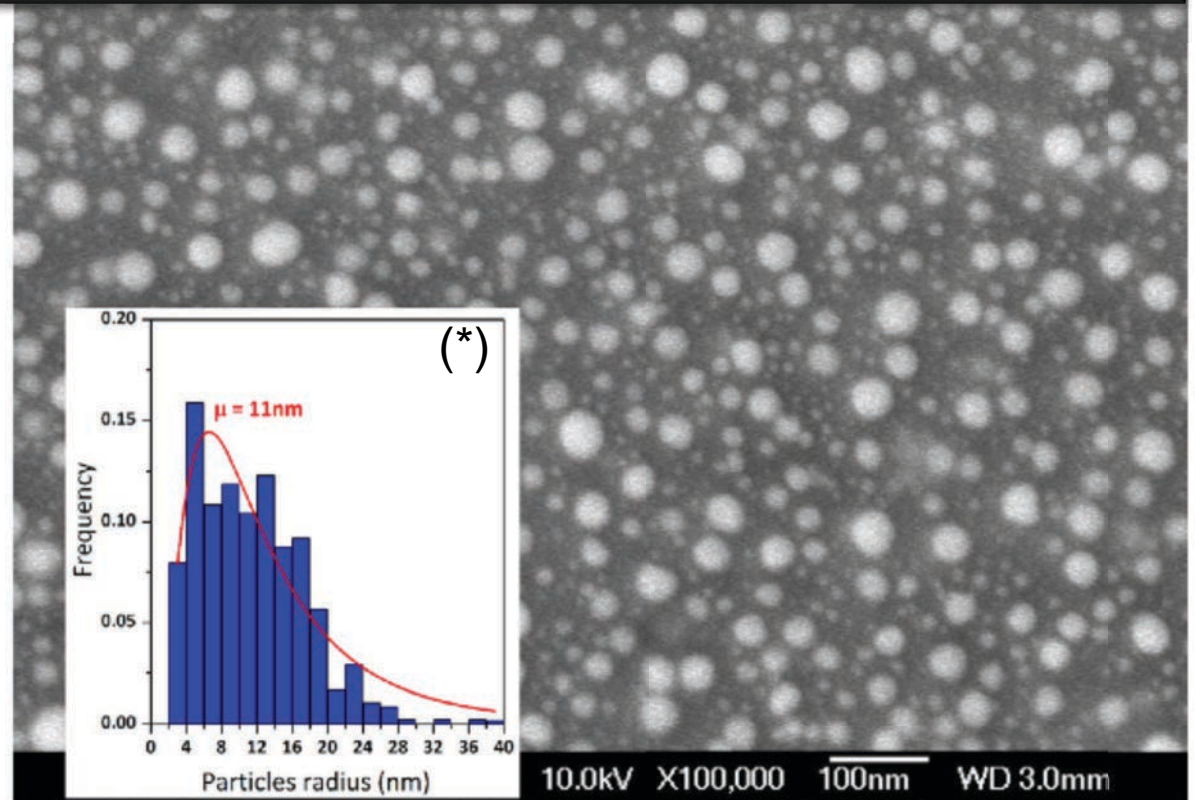
n_j^* : number of j-sized NPs

$$\tau = \int_0^t 16\pi R_1^2 \cdot \left(\frac{kT(t')}{\pi m_1} \right)^{\frac{1}{2}} \cdot \frac{N}{V(t')} dt'$$

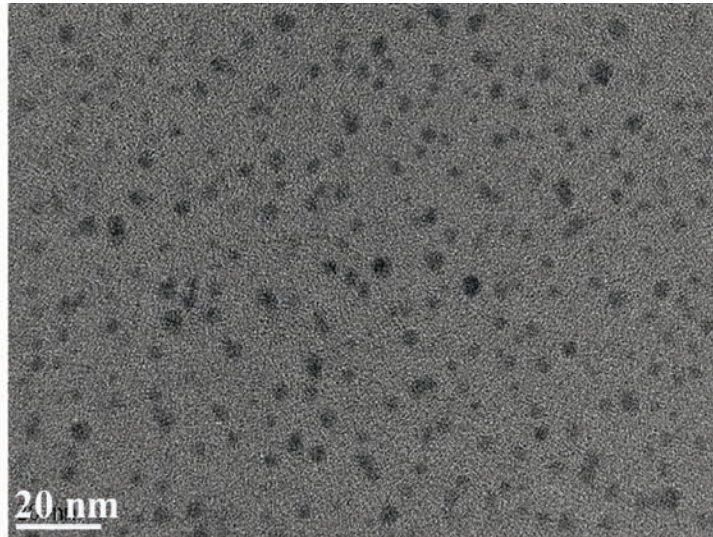
NP size distribution fct of a single parameter: condensation rate τ



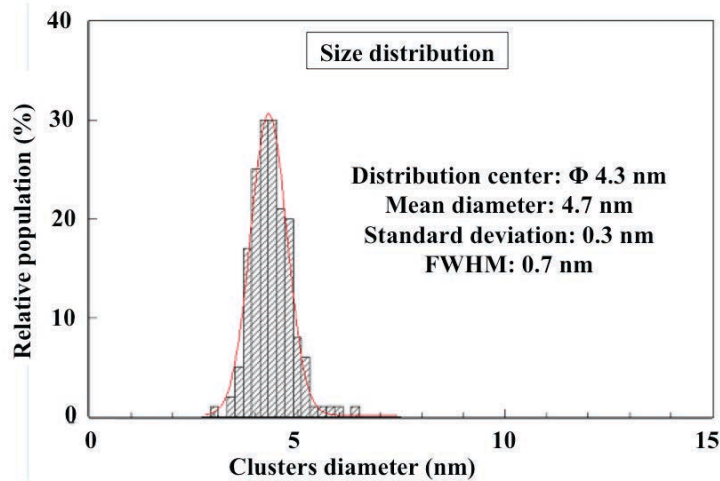
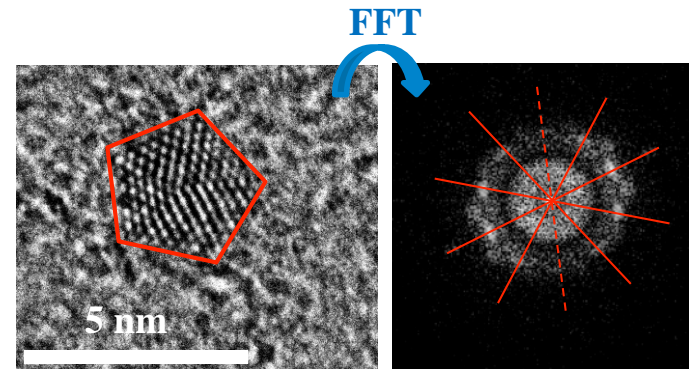
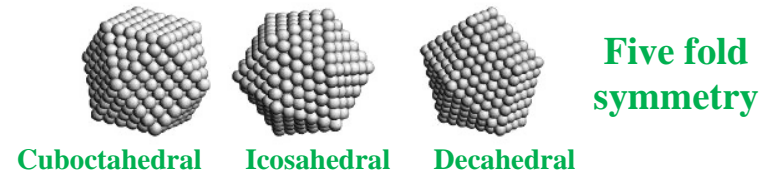
NP examples - Nanostructures



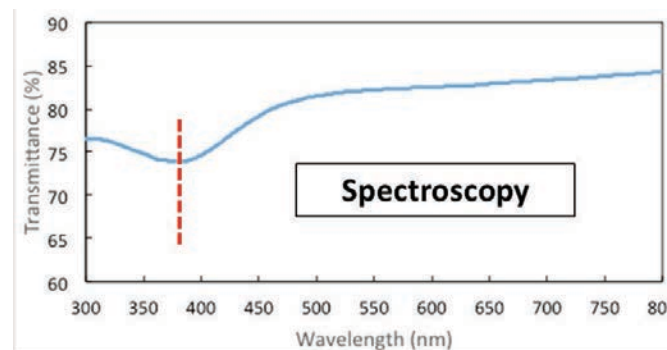
Silver nanoparticles



HR-TEM image of Silver NPs embedded in amorphous C-matrix



NP's **Narrow** size distribution



Surface Plasmon Resonance of silver at $\lambda = 379$ nm

NP's keep their **metallic nature**

NP growth: homogeneous nucleation theory

Kinetic equations for NP-NP reactions:

$$\frac{dn_k^*}{d\tau(t)} = \sum_{\substack{i+j=k \\ i \leq j}} C_{ij}^* \cdot n_i^* \cdot n_j^* - \sum_i C_{ik}^* \cdot n_i^* \cdot n_k^*$$

Formation rate of k-sized NP resulting from the coalescence of a i-NP and a j-NP

Number of events where k-sized NPs form bigger NPs

C_{ij} : coalescence probability between a i-NP and a j-NP

$n_i^* = \frac{N_i}{N}$ reduced variable

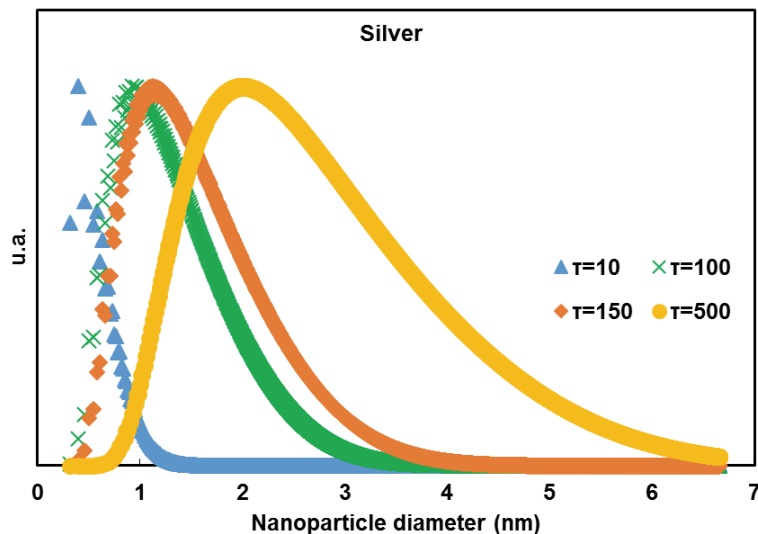
n_i^* : number of i-sized NPs

n_j^* : number of j-sized NPs

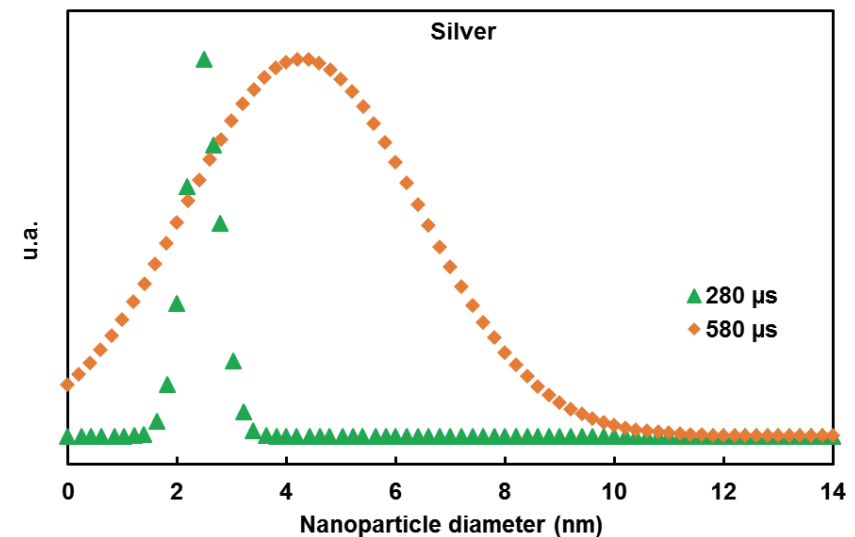
NP size distribution fct of a single parameter: condensation rate τ

$$\tau = \int_0^t 16\pi R_1^2 \cdot \left(\frac{kT(t')}{\pi m_1} \right)^{\frac{1}{2}} \cdot \frac{N}{V(t')} dt'$$

Theoretical

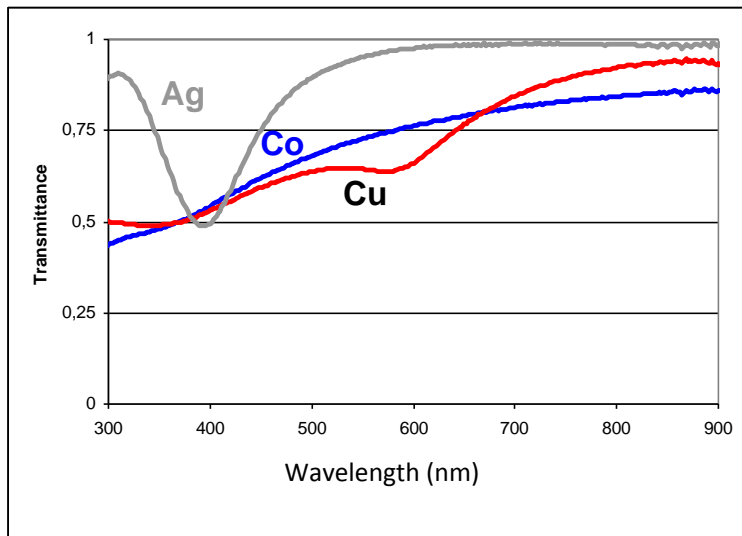
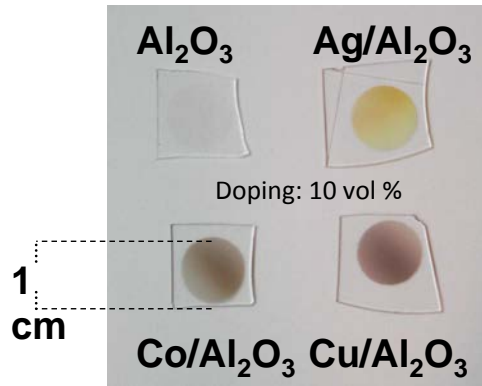


Experimental (data collected from TEM images)



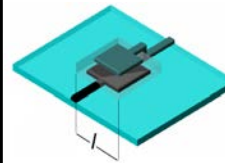
Ag, Co, Cu- NPs in PLD-Al₂O₃ matrix

Optical properties



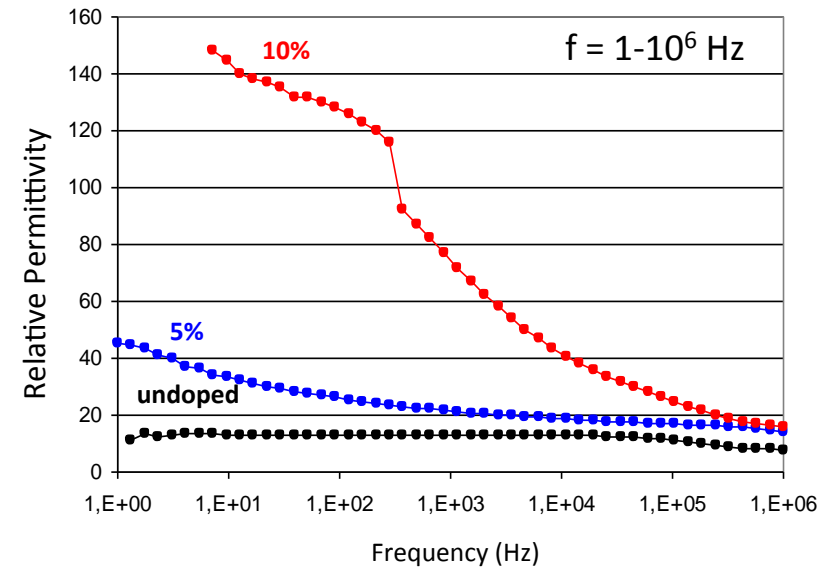
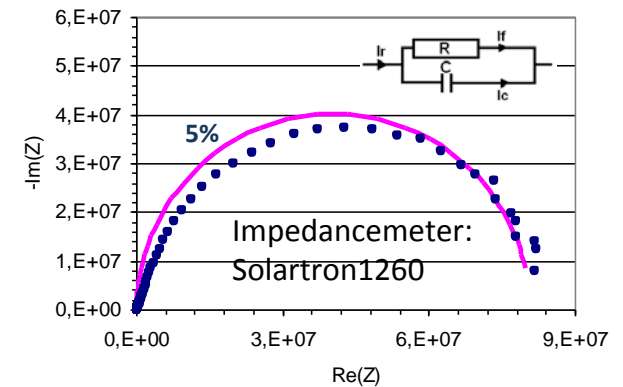
Electrical properties*

MIM structure

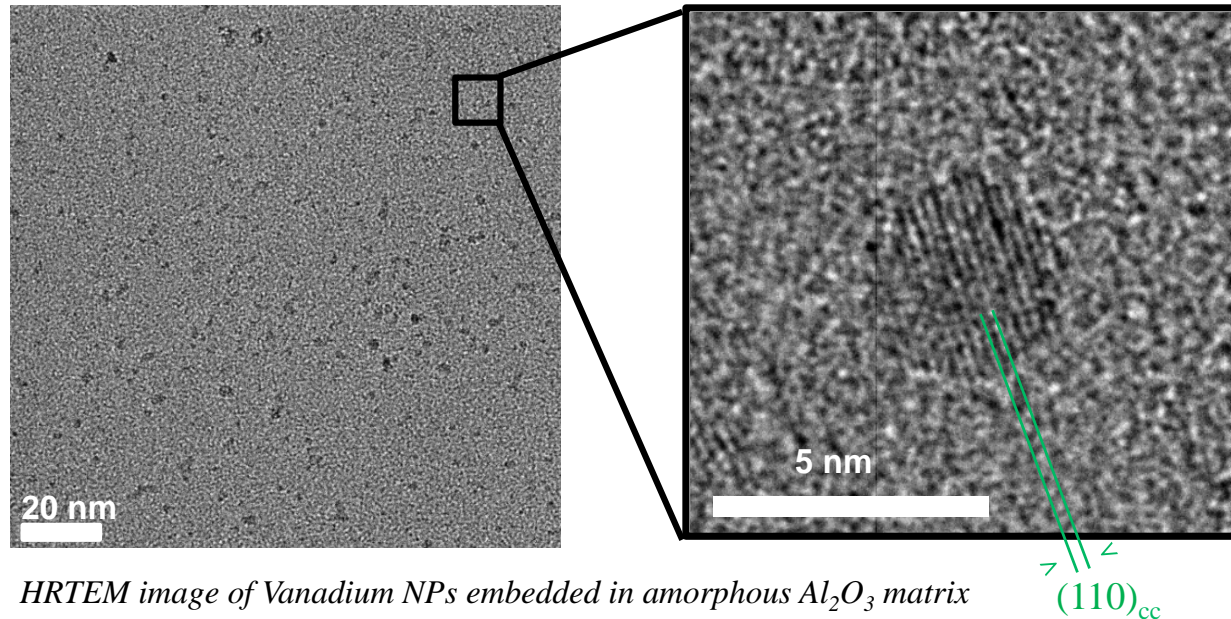


$$C = \epsilon_r \cdot \epsilon_0 \cdot \frac{S}{d}$$

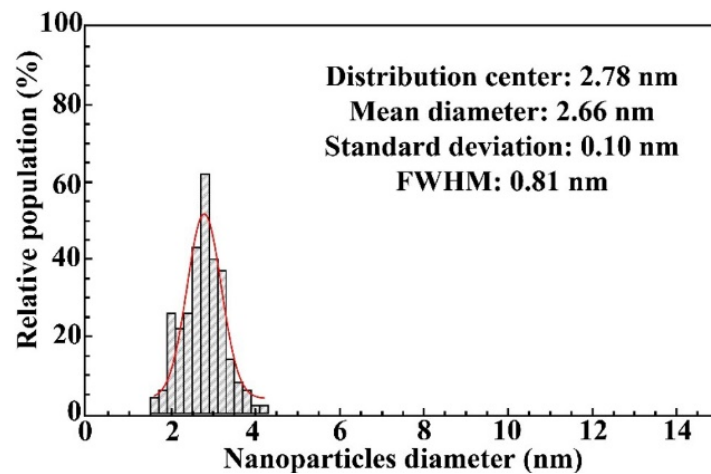
$$Z_t = \frac{R}{1 + R^2 \cdot C^2 \cdot \omega^2} - j \frac{R^2 \cdot C \cdot \omega}{1 + R^2 \cdot C^2 \cdot \omega^2}$$



*Crunteanu, Dumas-Bouchiat, Champeaux, Catherinot, Blondy, Thin Sol. Films 16 (2007)



HRTEM image of Vanadium NPs embedded in amorphous Al_2O_3 matrix

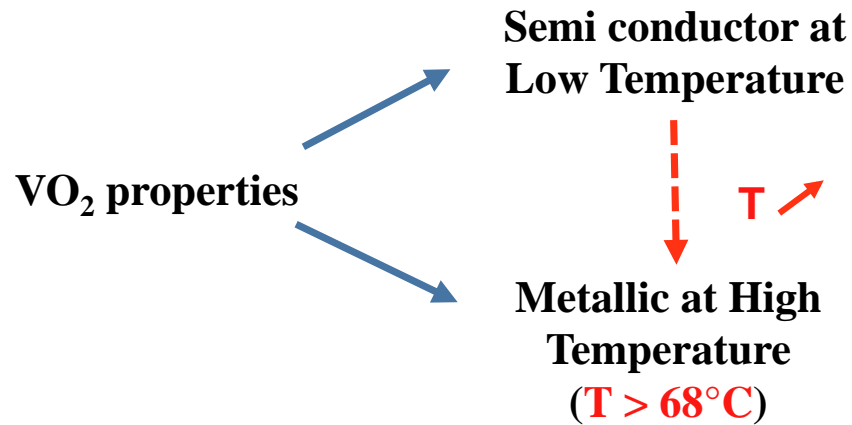


↳ NPs well **crystallised** in **cc** structure **at RT**

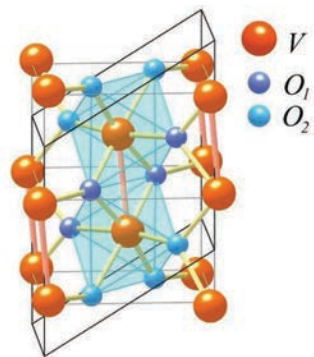
- **Crystallised ~3 nm metallic NPs at RT, sharp size distribution**
- **High deposition rate (50 nm of V-NPs per 15 min)**
- **Flexible choice of materials:**
 - Isolated NPs embedded in different matrix
 - Stacks of NPs (porosity properties)

Vanadium dioxide (VO₂) thermochromic mat.

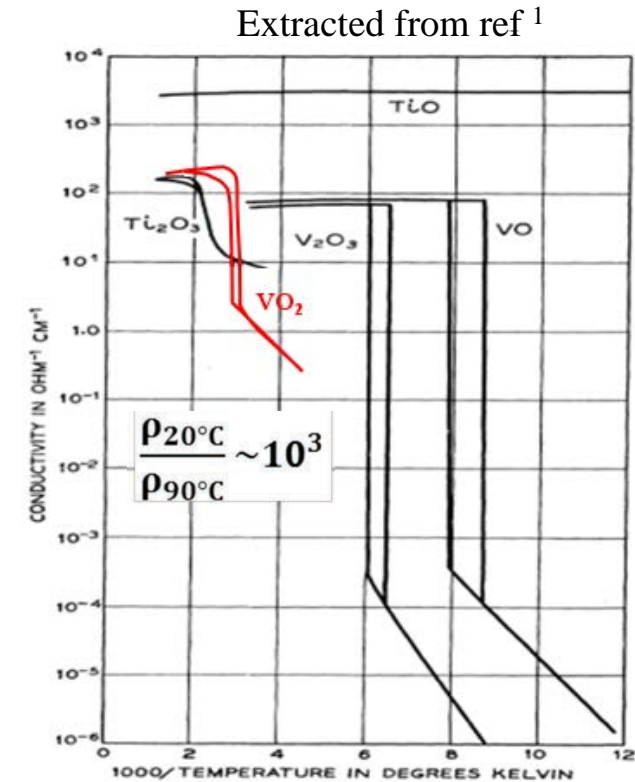
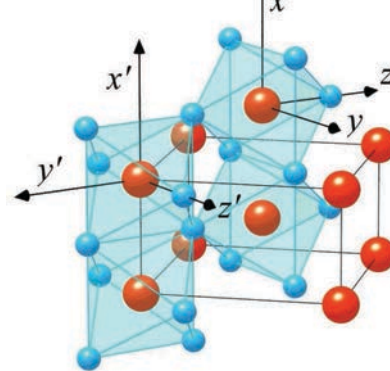
Reversible first order Insulator to Metal Transition at ~68°C (close to RT)



Monoclinic phase



Rutile phase



↳ Abrupt changes in electrical resistivity and optical properties (IR range)

¹J.F. Morin, *Physical Review Letters*, 1959

Nanosized VO₂ NPs vs VO₂ PLD thin films

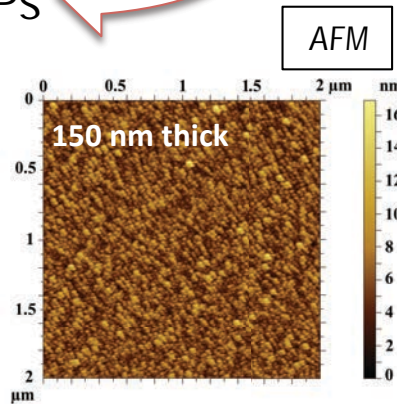
13^{ème} Journées – Réseau Plasmas Froids – La Rochelle – 17-20 octobre 2016

V NPs

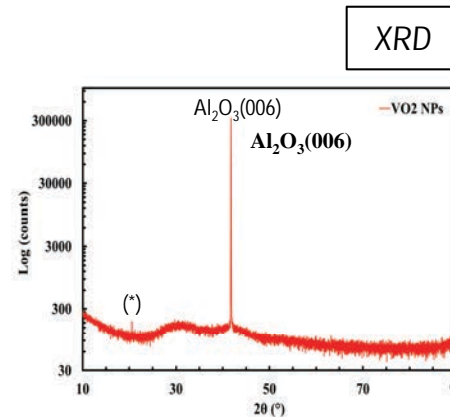


VO₂ NPs

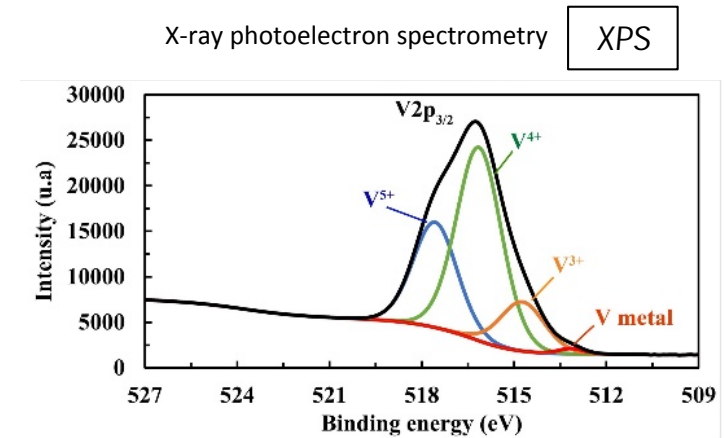
post annealing @ 300°C, P_{O₂}: 3.3.10⁻² mbar, Al₂O₃, MgO or Glass substrate



AFM



XRD



X-ray photoelectron spectrometry

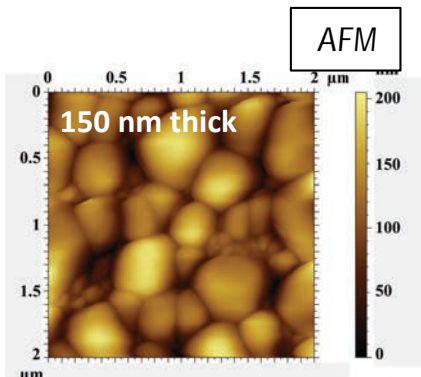
XPS

Only substrate peaks
No peak of VO₂; no long range order

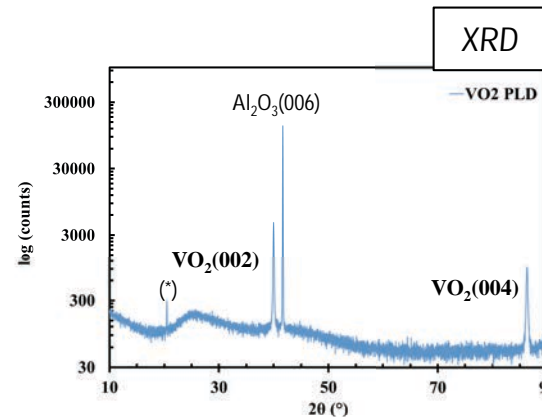
VO₂ major phase

PLD VO₂ thin film

deposited at 700°C, P_{O₂}: 2.2.10⁻² mbar, Al₂O₃ substrate



AFM

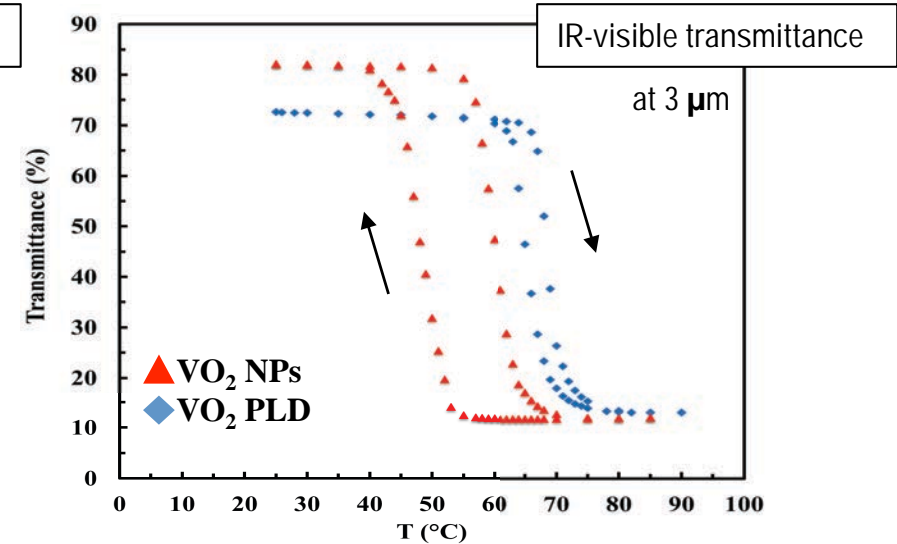
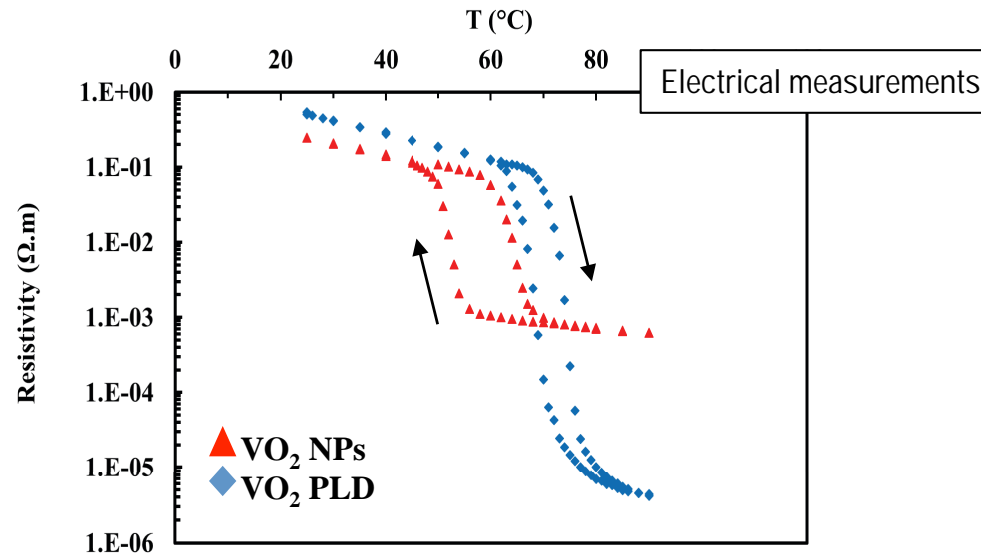


XRD

- well cristallized mono-oriented
(020) VO₂ film

~150-200 nm sized grains

Nanosized VO₂ NPs vs VO₂ PLD thin films¹



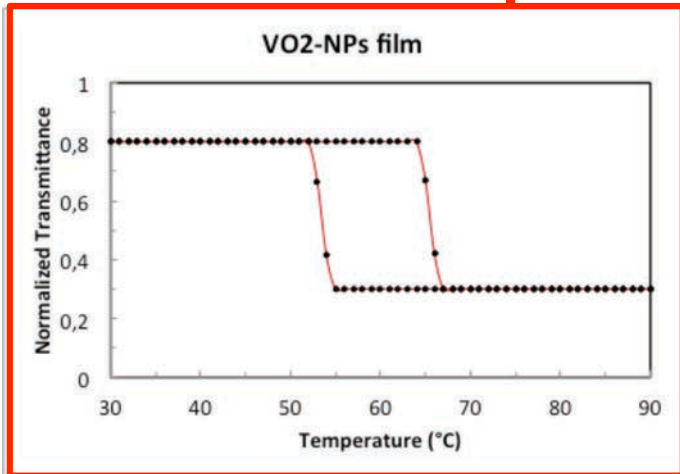
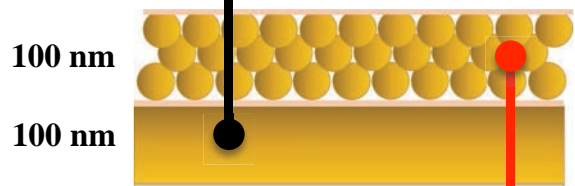
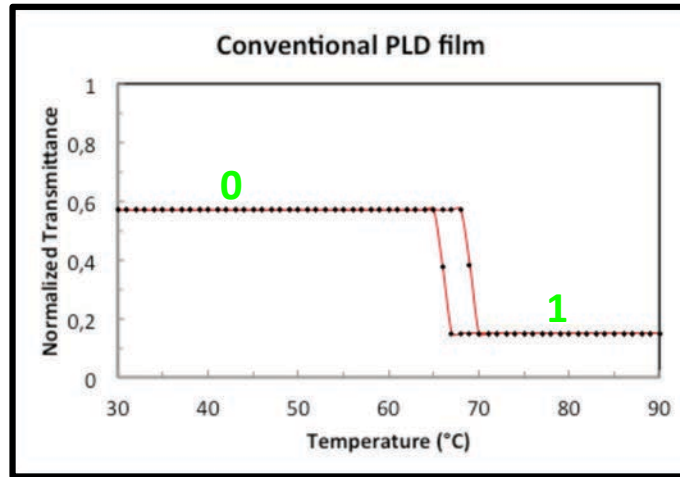
Measurement	T _c (°C)	ΔT(°C)	ΔA
VO ₂ NPs			
Transmittance	54	12	8
Resistivity	58	12	4.10 ²
VO ₂ PLD			
Transmittance	68	3	5.5
Resistivity	72	5	1.10 ⁵

NPs vs dense films
 - Increase of hysteresis width
 - Decrease of T_{MIT}

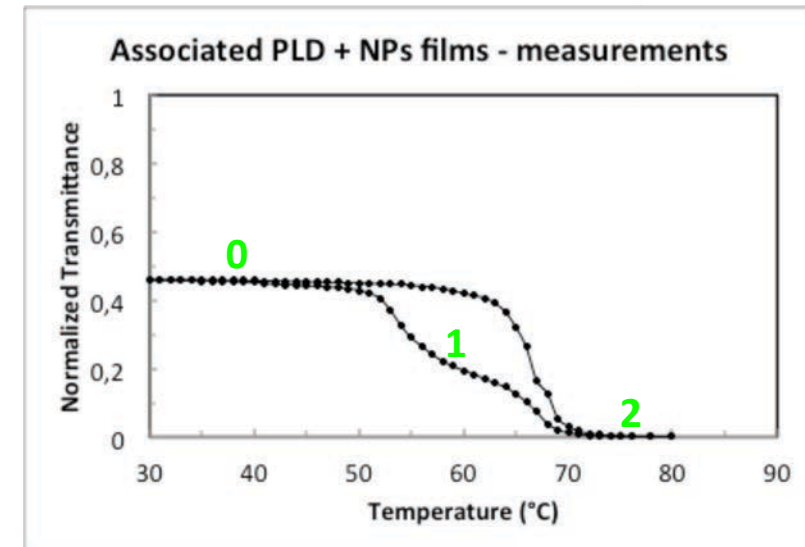
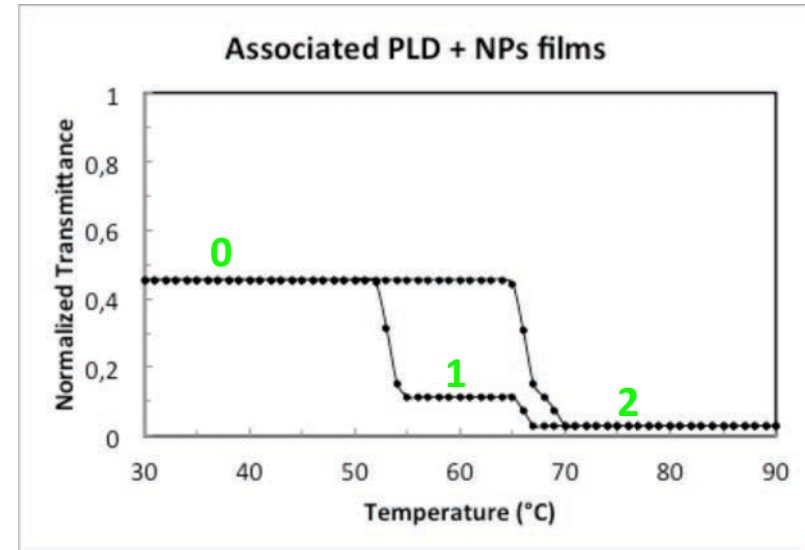
¹ANR Project MUFRED 2017-2019: VO₂ integration in microsystems:
 SPCTS, Xlim Limoges, LMGP Grenoble, IETR Rennes, Thales Paris, Lab-STICC Brest

Combine VO₂ NPs & VO₂ PLD thin films

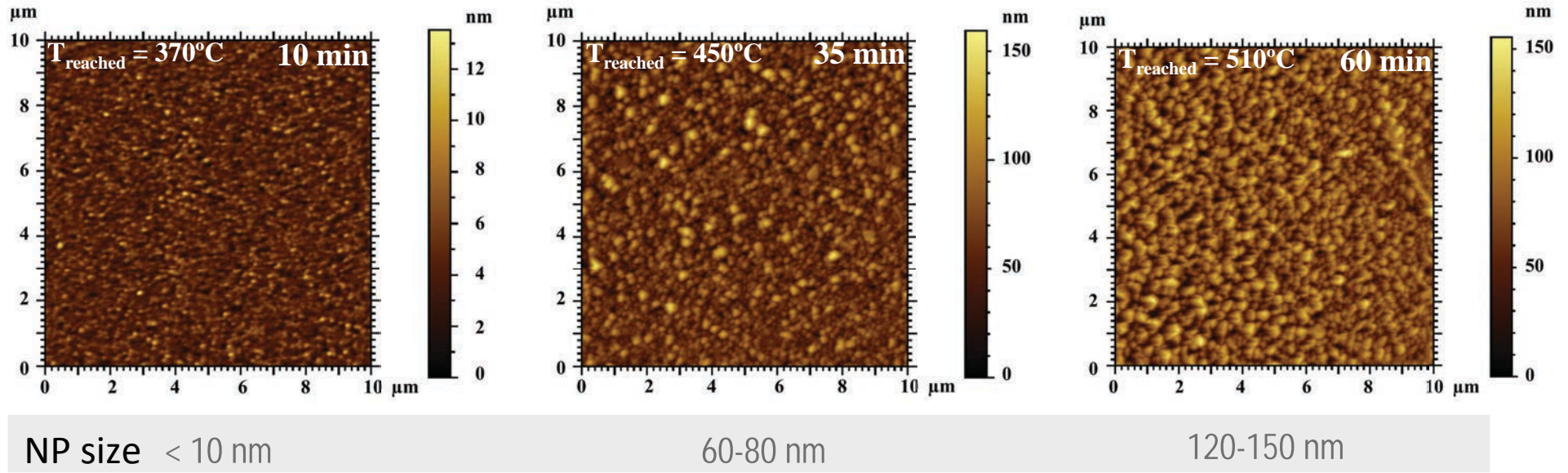
$T_{max}=0.57$, $T_{min}=0.15$, $T_{transition}=68^{\circ}\text{C}$, hysteresis width: 2°C



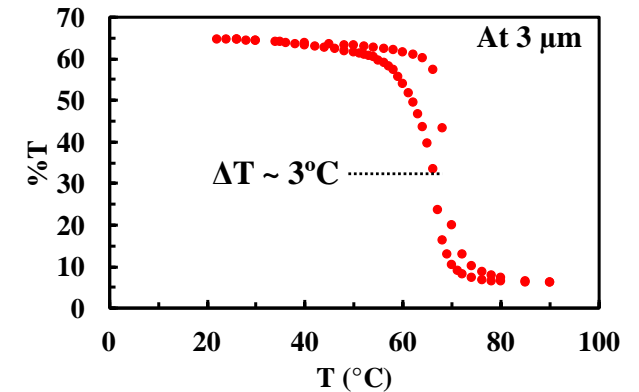
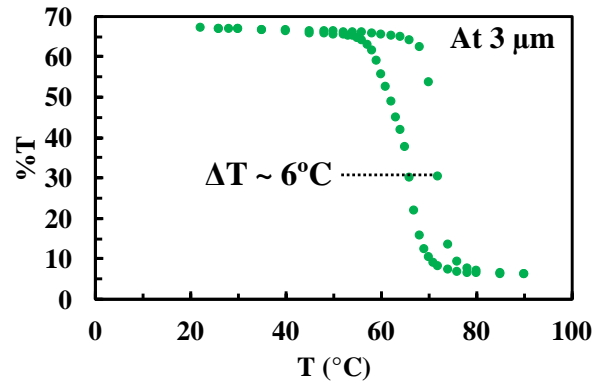
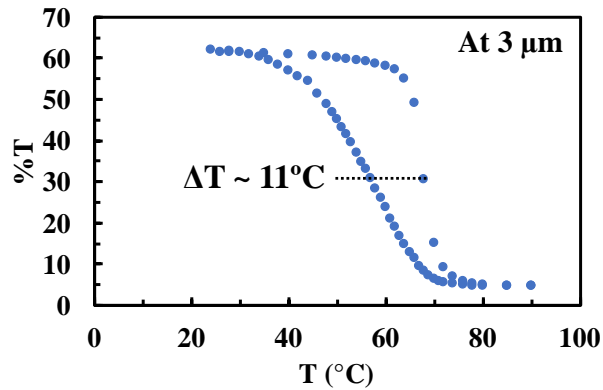
$T_{max}=0.80$, $T_{min}=0.20$, $T_{transition}=60^{\circ}\text{C}$, hysteresis width: 10°C



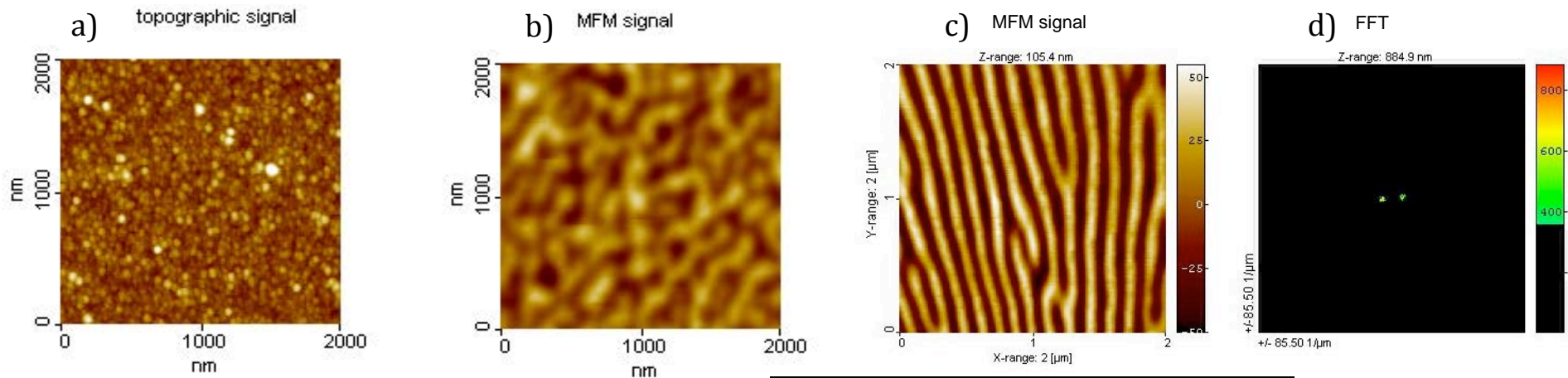
Nanocomposite: VO₂ NPs/Thin films



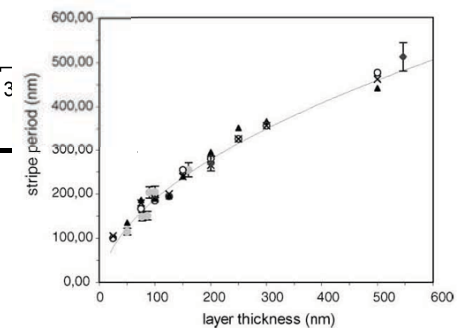
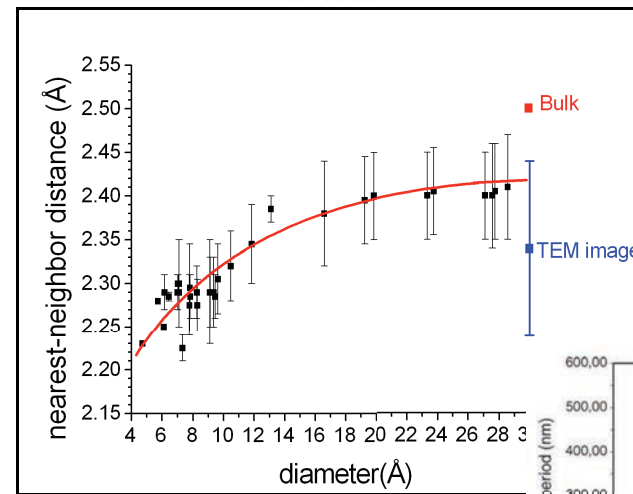
↪ Coalescence and NPs growth observed with annealing time



Cobalt NPs: stacking



- ↪ Contraction of the crystal lattice¹
- ↪ Exhibition of a \sqrt{t} dependance²
- ↪ Chudnovsky model: magnetic entity 9nm^3



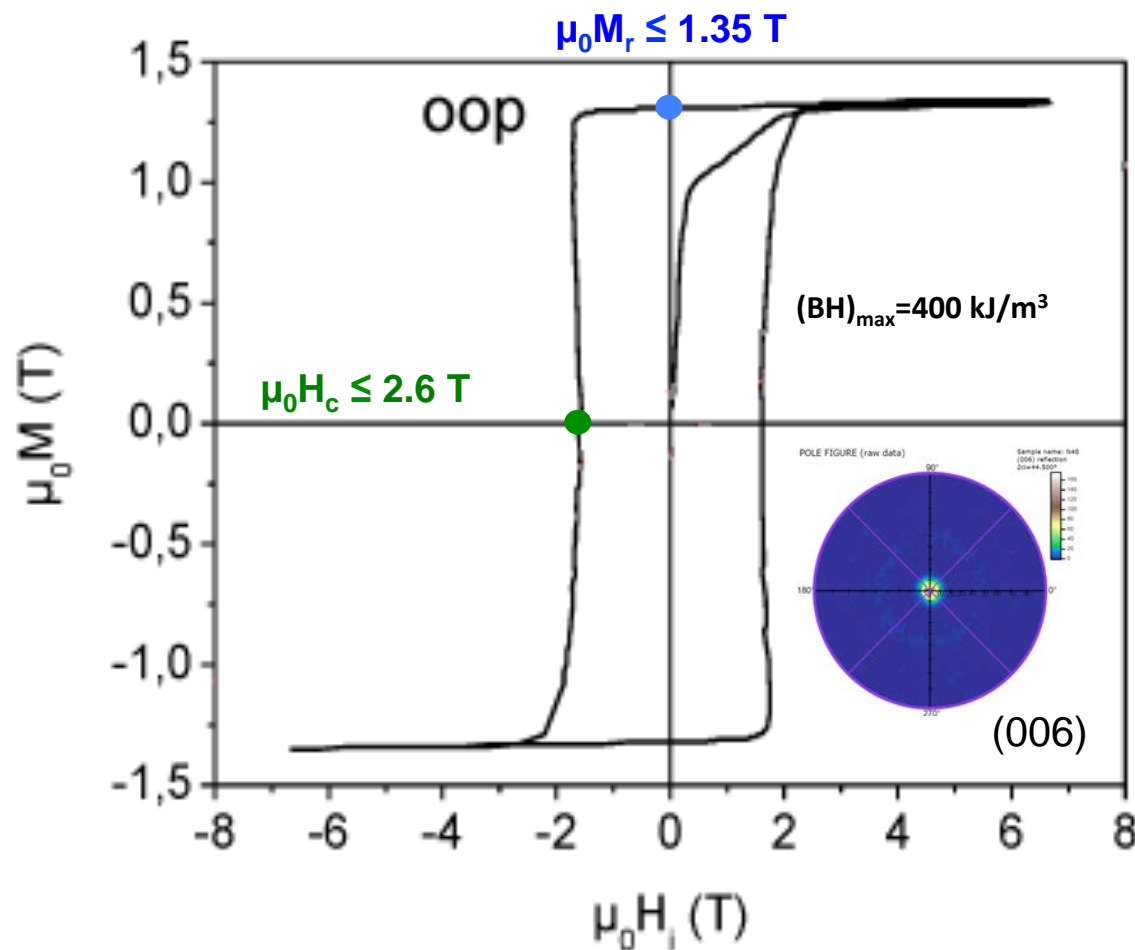
¹Rives, *Phys. Rev. B* 77 (2008)

²Dumas-Bouchiat, *Appl. Surf. Sci.* 247 (2005)

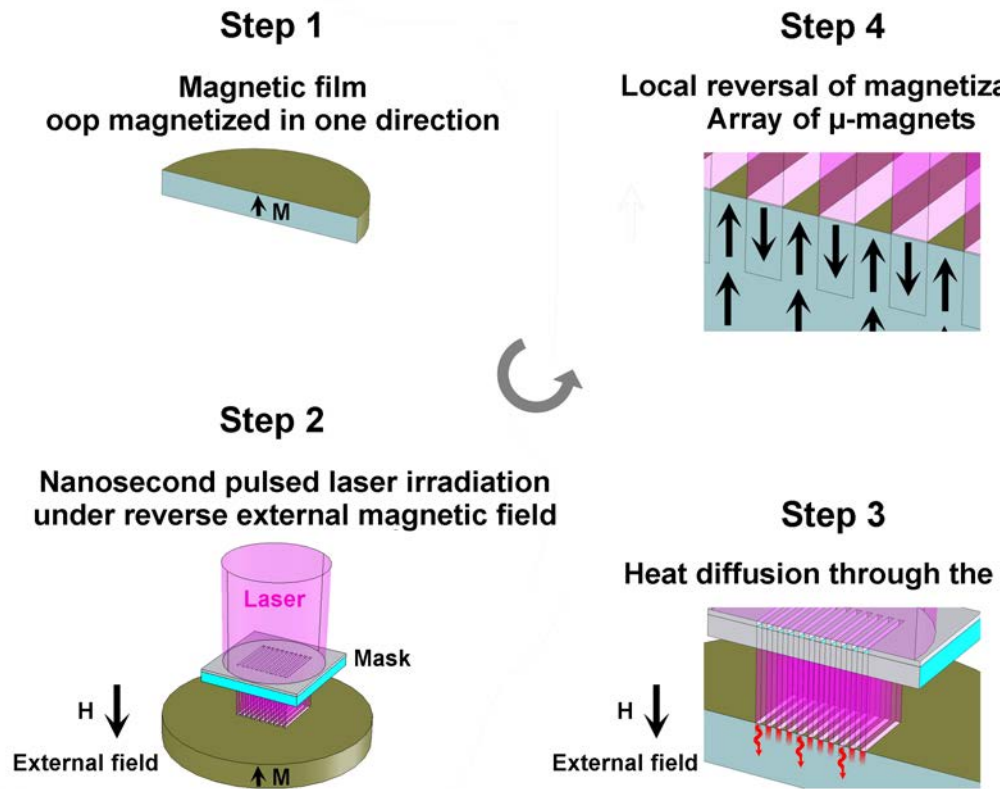
³Dumas-Bouchiat, *J. Appl. Phys.* 100 (2006)

Applications, playing with magnetic NPs ...

Hard magnetic film Grenoble/institut Neel/ N.M. Dempsey



Focus on Thermo-Magnetic Patterning: TMP



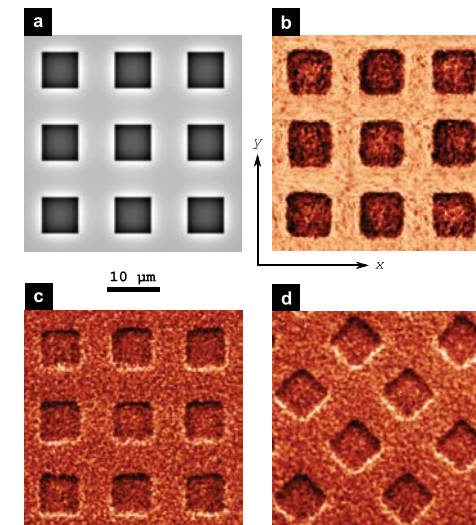
- ↪ Laser fluence adapted not to damage the film
- ↪ Magnetisation reversed on $1.5 \mu\text{m}$

IEEE Front Cover, sept 2016

IEEE TRANSACTIONS ON MAGNETICS

A PUBLICATION OF THE IEEE MAGNETICS SOCIETY

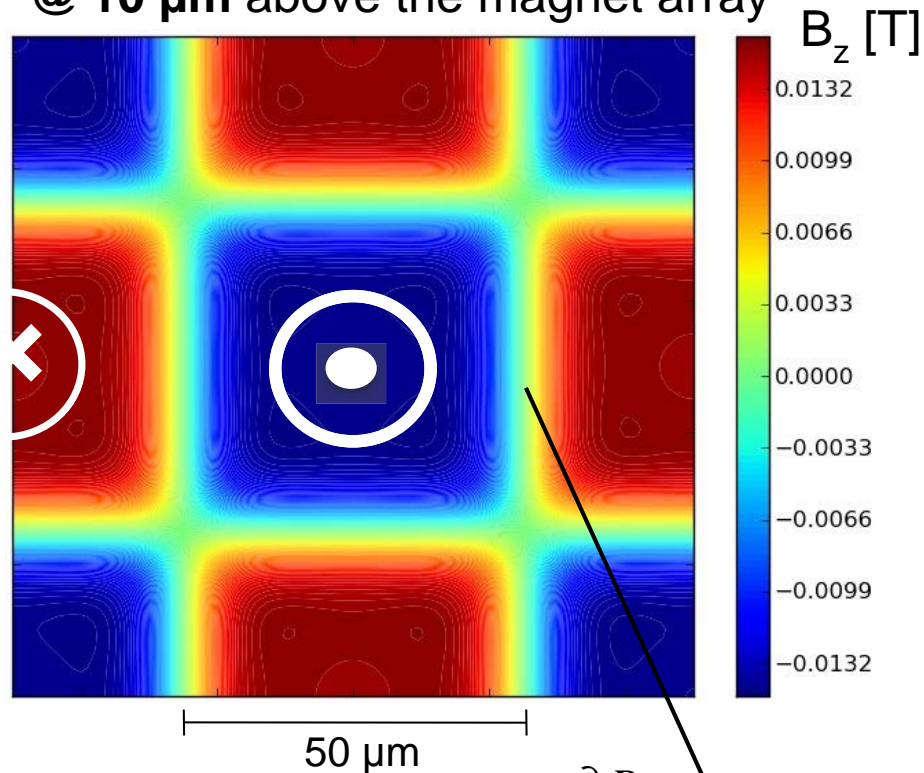
SEPTEMBER 2016 VOLUME 52 NUMBER 9 IEMGAQ (ISSN 0018-9464)



(a) Calculated map of the vertical component of the stray field at a height of 100 nm above the patterned SmCo film. (b) Phase shift map measured with a flexible cantilever soft coating probe. (c) and (d) Phase shift maps measured with a stiff cantilever hard coating probe. From the paper, "Some Aspects of Magnetic Force Microscopy of Hard Magnetic Films;" by G. Ciuta *et al.*, Art. no. 6500408.

Magnetic stray fields & forces

Z-component of the magnetic stray field
@ 10 μm above the magnet array



$$\frac{\partial B}{\partial z} = 10^6 \text{ T/m @ } 2 \text{ nm}$$

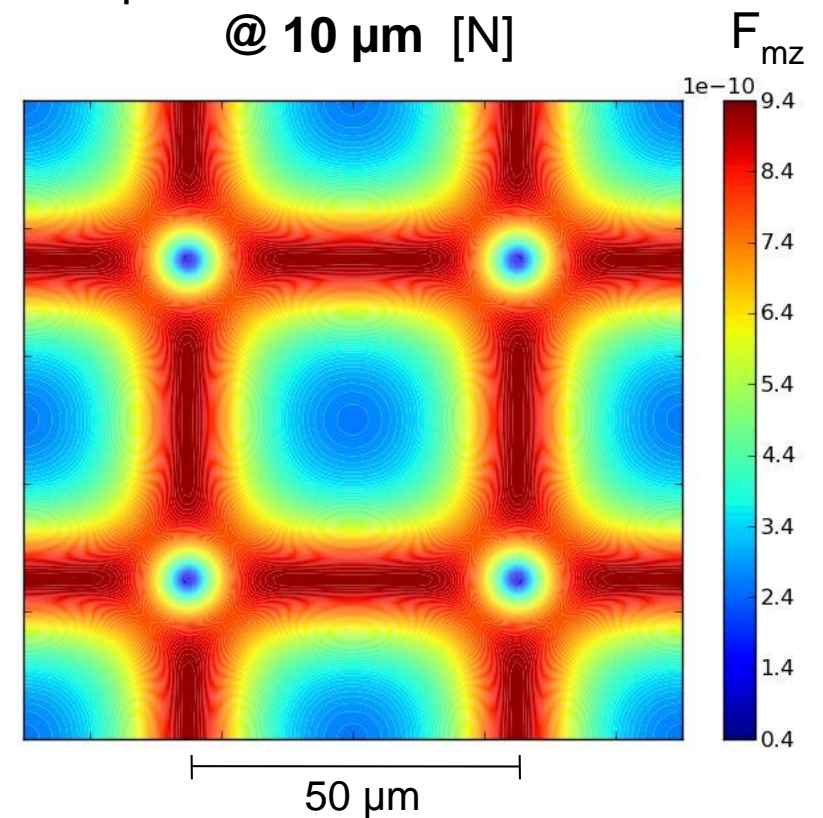
@ 10 μm above

↖ Magnetic field → tens of mT

↖ Magnetic trapping force → hundreds of pN

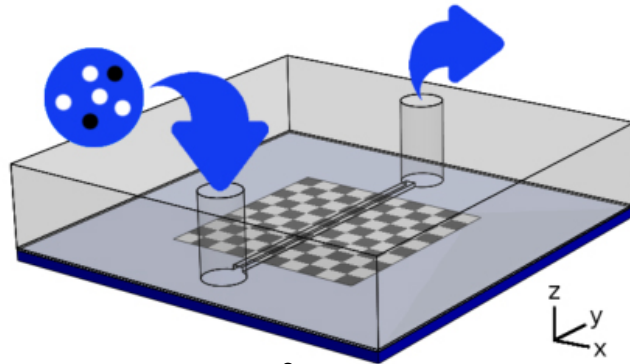
Superparamagnetic NPs \varnothing 3 μm
20 % wt Fe_3O_4 80 % wt Polystyrene

Z-component of the attraction force
@ 10 μm [N]



Microfluidic potential: NPs sorting

μ -fluidic channel in PDMS, width = 500 μm , t_{PDMS} on film $\approx 10 \mu\text{m}$

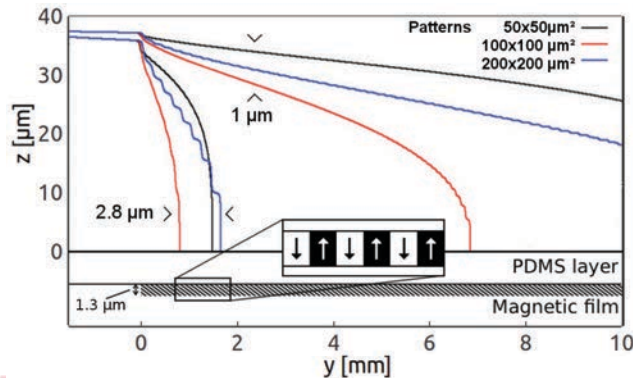


NPs sorting by trapping

$$F_g = \frac{4}{3} \pi r_{\text{bead}}^3 (\rho_{\text{bead}} - \rho_{\text{medium}}) g$$

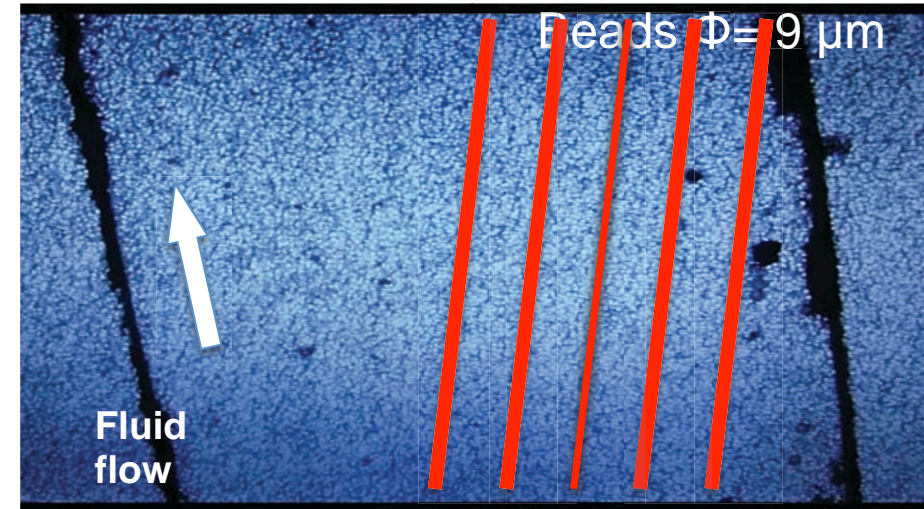
$$F_d = 6 \pi \eta r_{\text{bead}} (u_{\text{fluid}} - u_{\text{bead}})$$

$$F_m = \mu_0 V_{\text{mag}} M \nabla H$$

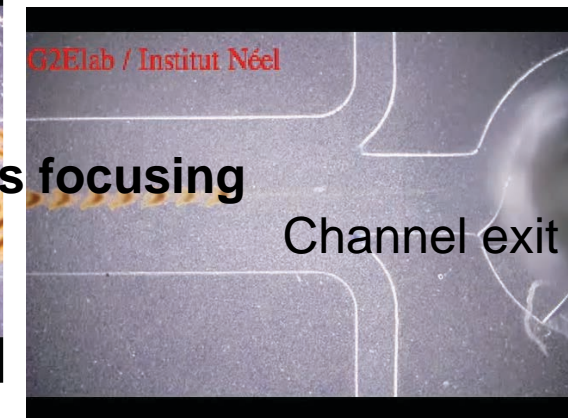
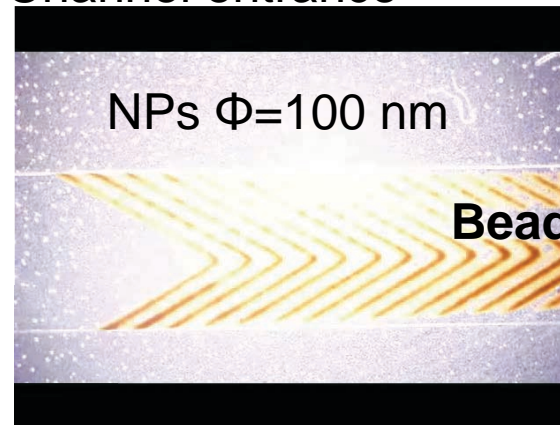


- ↖ No external magnetic field
- ↖ No power source
- ↖ Stray fields restric. to the region of interest
- ↖ Adapted to space restricted (microscopy)

NPs sorting by guiding: Dynamic mode

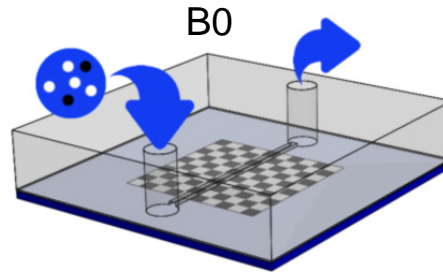


Channel entrance

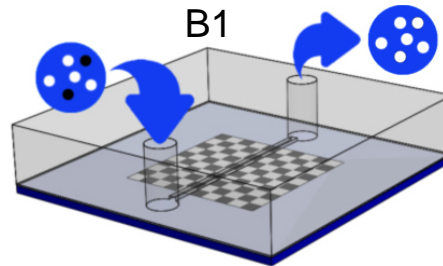


High gradient magnetic separation-HGMS

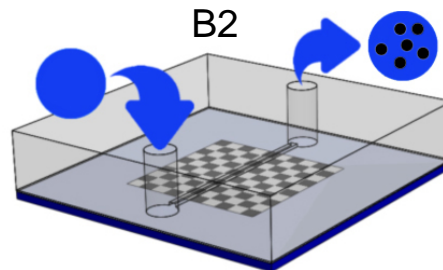
B0: initial composition
65.6% PS NPs
34.4% Magnetic NPs



After a first pass through the channel
 B1: selected solution
99.9% PS NPs

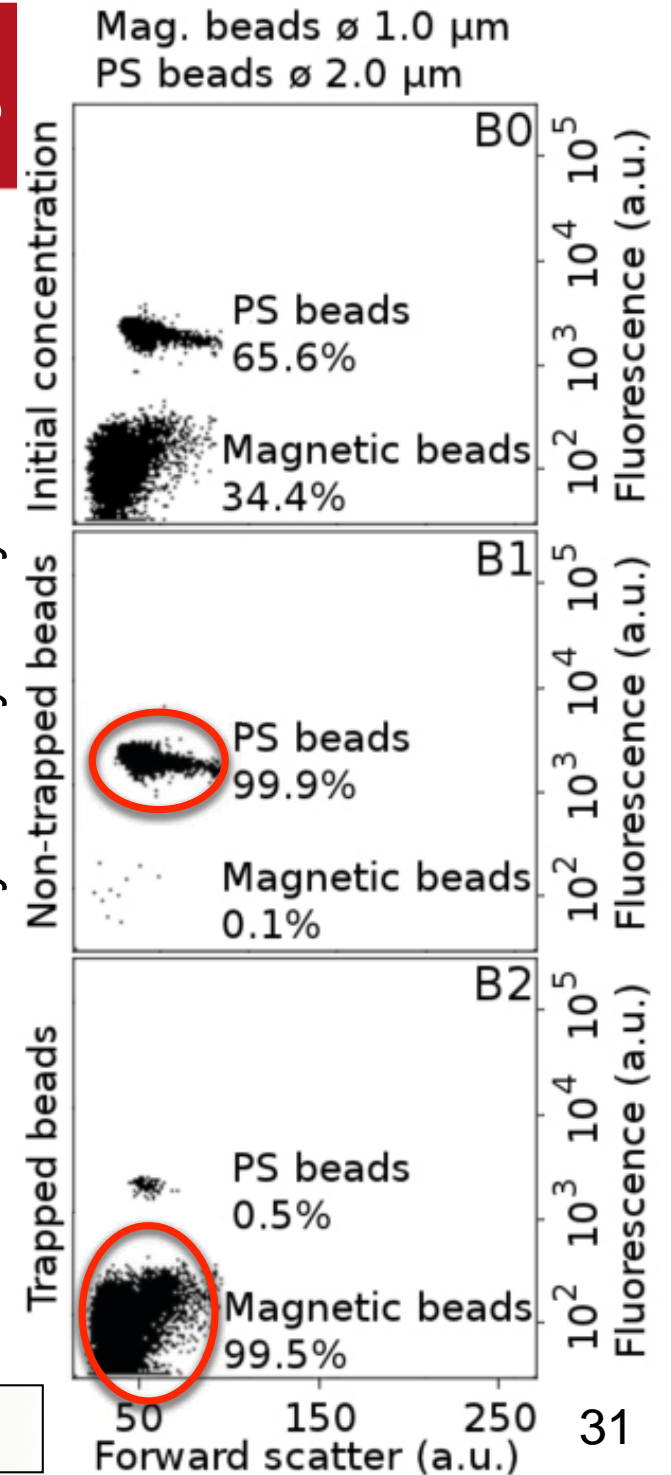


high fluid flow to clean the channel
 B2: solution with magnetic beads
99.5% Magnetic NPs



- ↪ Highly efficient for NPs
- ↪ Highly efficient for tag Cells (Jurkat & HEK) 95% / 5%

Flow cytometry analysis

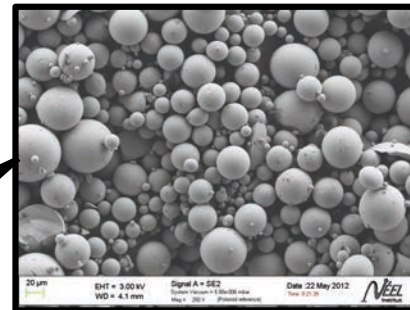
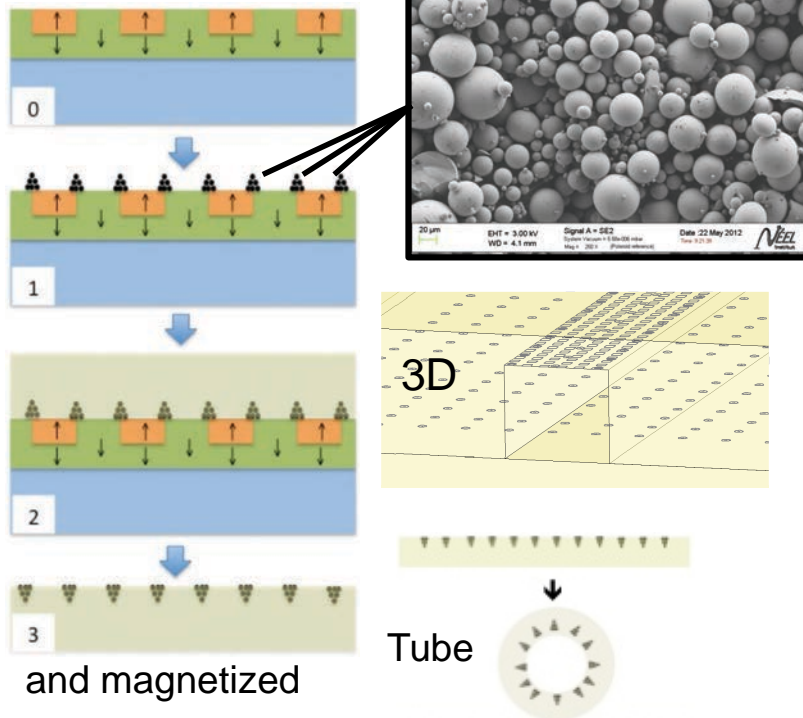


μ -magnetic imprinting MMI, N.M. Dempsey

- 0 - TMP structure
- 1 - Hard magnetic beads sprinkled onto master structure and concentrated at the interfaces of micro-magnets
- 2 - polymer binder poured over the hard magnetic beads
- 3 - Solid composite peeled off the master structure

Magnequench® NdFeB powders GA50

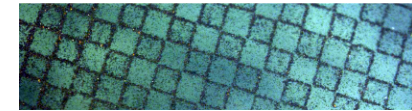
MMI



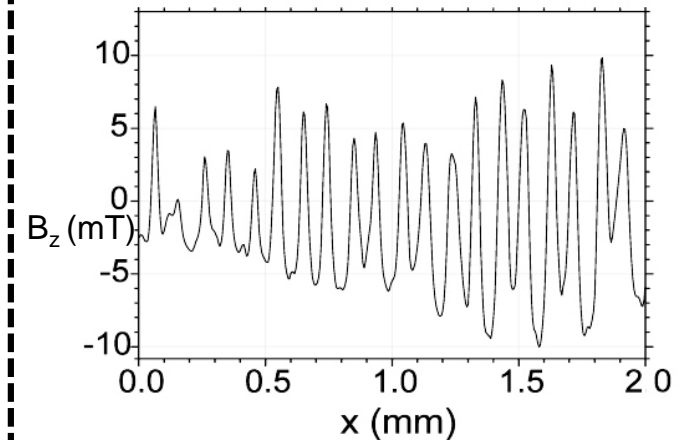
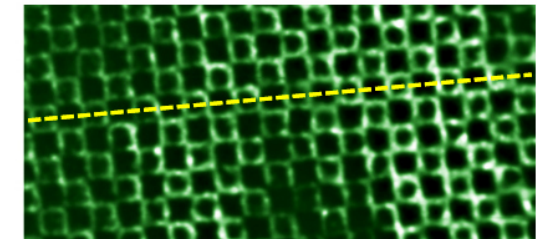
- Cheap
- Flexible
- Transparent
- Biologically compatible
- One Master for thousands prototypes

Example of magn. polymer structures

Optical image



Scanning μ -Hall probe



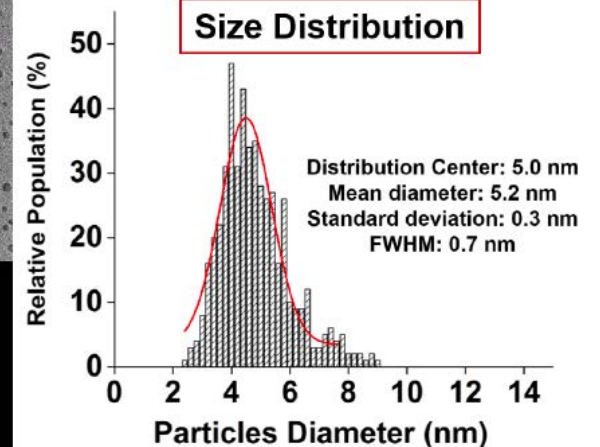
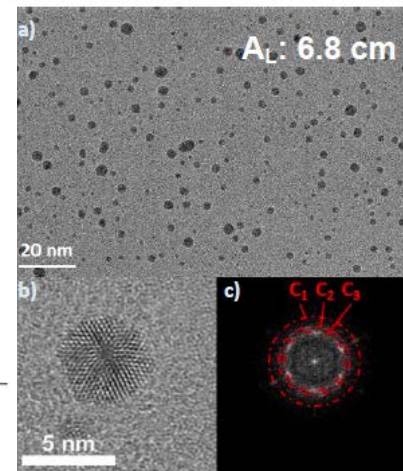
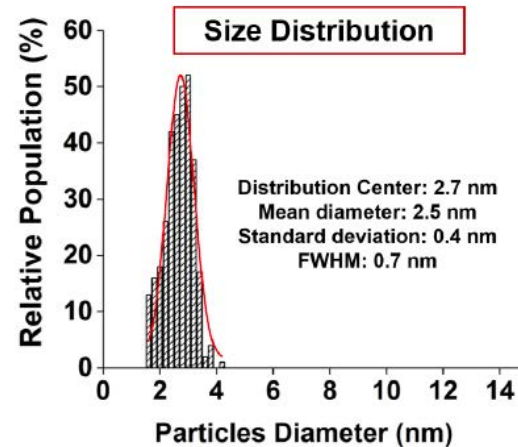
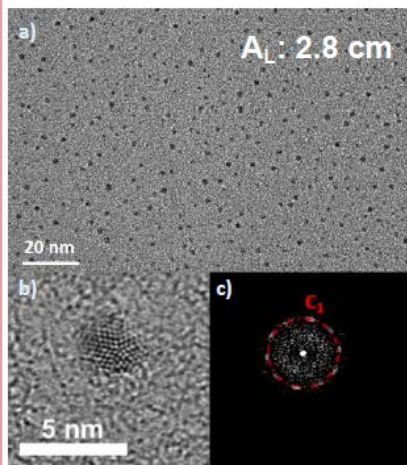
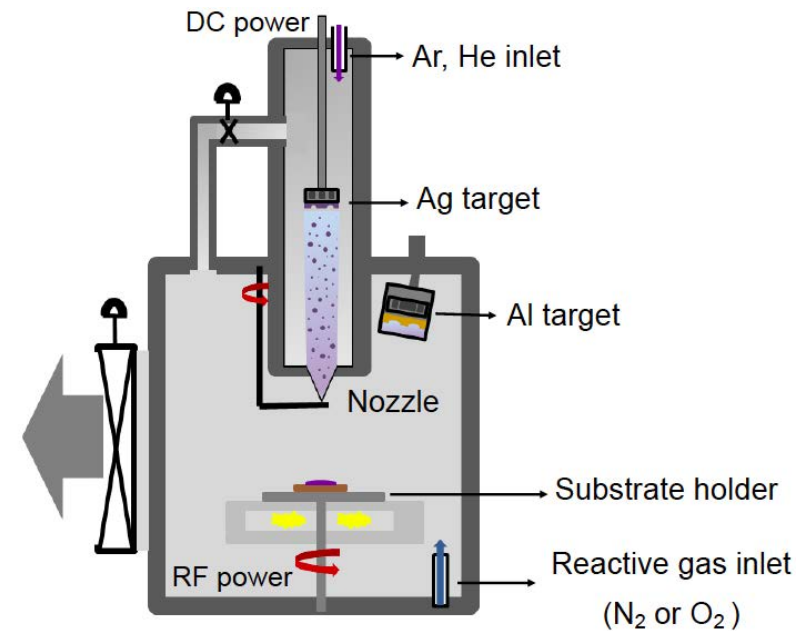
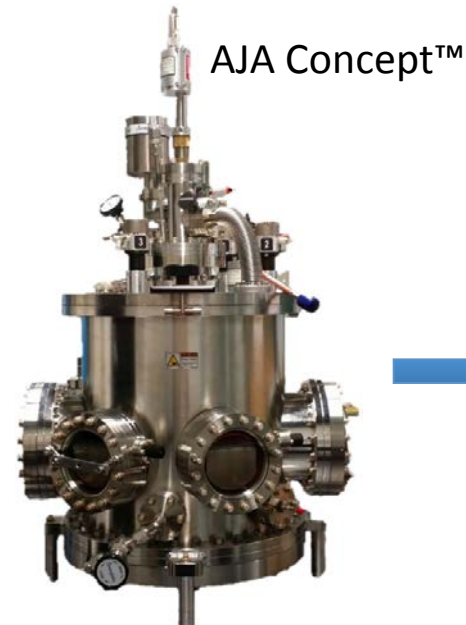
Extract the B_z magnitude

Other Free NP sources

Vanessa Orozco Montes, Cedric Jaoul, Pascal Tristant

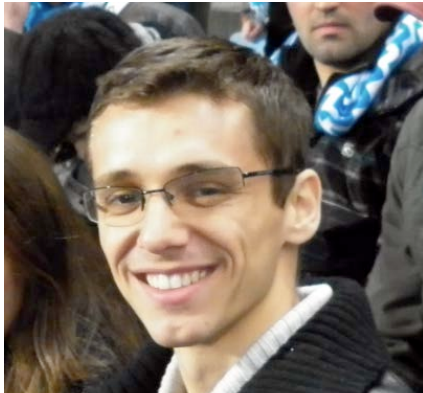
Limoges Free NP source based on magnetron sputtering

Poster: Optical Emission Spectroscopy



Many thanks to students and especially:

2009-2012



Luiz Fernando Zanini



2013-2016



Michael Gaudin



2014- ...



Maileth Vanessa Orozco Montes



frederic.dumas-bouchiat@unilim.fr



Science des Procédés Céramiques
et de Traitements de Surface

Thank you for your attention

